

AD-A087 218

AD A 087 218

IA-80-0347

AD

TECHNICAL REPORT ARLCB-TR-80010

TECHNICAL
LIBRARY

STRESS CONCENTRATIONS IN SCREW THREADS

G. P. O'Hara

April 1980



US ARMY ARMAMENT RESEARCH AND DEVELOPMENT COMMAND
LARGE CALIBER WEAPON SYSTEMS LABORATORY
BENET WEAPONS LABORATORY
WATERVLIET, N. Y. 12189

AMCMS No. 4111.16.2991.6

PRON No. 1A-9-39362-Y

APPROVED FOR PUBLIC RELEASE; DISTRIBUTION UNLIMITED

DISCLAIMER

The findings in this report are not to be construed as an official Department of the Army position unless so designated by other authorized documents.

The use of trade name(s) and/or manufacturer(s) does not constitute an official indorsement or approval.

DISPOSITION

Destroy this report when it is no longer needed. Do not return it to the originator.

REPORT DOCUMENTATION PAGE		READ INSTRUCTIONS BEFORE COMPLETING FORM
1. REPORT NUMBER ARLCB-TR-80010	2. GOVT ACCESSION NO.	3. RECIPIENT'S CATALOG NUMBER
4. TITLE (and Subtitle) STRESS CONCENTRATIONS IN SCREW THREADS		5. TYPE OF REPORT & PERIOD COVERED
		6. PERFORMING ORG. REPORT NUMBER
7. AUTHOR(s) G. P. O'Hara		8. CONTRACT OR GRANT NUMBER(s)
9. PERFORMING ORGANIZATION NAME AND ADDRESS US Army Research and Development Command Benet Weapons Laboratory, DRDAR-LCB-TL Watervliet N.Y. 12189		10. PROGRAM ELEMENT, PROJECT, TASK AREA & WORK UNIT NUMBERS AMCMS No. 4111.16.2991.6 PRON No. 1A-9-39362-Y
11. CONTROLLING OFFICE NAME AND ADDRESS US Army Armament Research and Development Command Large Caliber Weapon Systems Laboratory Dover, New Jersey 07801		12. REPORT DATE March 1980
		13. NUMBER OF PAGES 41
14. MONITORING AGENCY NAME & ADDRESS (if different from Controlling Office)		15. SECURITY CLASS. (of this report) UNCLASSIFIED
		15a. DECLASSIFICATION/DOWNGRADING SCHEDULE
16. DISTRIBUTION STATEMENT (of this Report) Approved for public release; distribution unlimited.		
17. DISTRIBUTION STATEMENT (of the abstract entered in Block 20, if different from Report)		
18. SUPPLEMENTARY NOTES Presented at the 8th NASTRAN Users' Colloquium, Goddard Space Flight Center, Oct 79. To be published in the proceedings of the 8th NASTRAN Users' Colloquium.		
19. KEY WORDS (Continue on reverse side if necessary and identify by block number) Failure Stress-Concentration Fatigue Lugs Screw-thread		
20. ABSTRACT (Continue on reverse side if necessary and identify by block number) The concept of stress concentration in screw threads is defined as a ratio of maximum fillet stress normalized to shear transfer rate. The data is presented as a plot of fillet stress vs. radial stress for a particular thread form. The Heywood equation is used to generate the basic plots and NASTRAN is used to extend the analysis to the case both where flanks of an individual thread tooth are in contact and the case where a finite axial stress is superimposed.		

SECURITY CLASSIFICATION OF THIS PAGE(When Data Entered)

SECURITY CLASSIFICATION OF THIS PAGE(When Data Entered)

TABLE OF CONTENTS

	<u>Page</u>
INTRODUCTION	1
THREAD GEOMETRY	4
LOADING PARAMETERS	6
HEYWOOD ANALYSIS	7
NASTRAN FINITE ELEMENT ANALYSIS	10
DISCUSSION	13
CONCLUSION	16
REFERENCES	17
APPENDIX A	18

TABLES

I. THREAD GEOMETRY DEFINITION	6
AI. THREAD GEOMETRY PARAMETERS	19

LIST OF ILLUSTRATIONS

1. Thread geometry and load parameters.	5
2. Heywood's equation.	8
3. Thread characteristic from Heywood analysis for:	9
1. British Standard Buttress	
2. Watervliet Buttress	
3. Controlled root "V"	
4. NASTRAN grid.	11
5. Thread characteristic curve - British Standard Buttress.	14
6. Thread characteristic curve - British Standard Buttress.	15
A1. Axial stress concentration thread characteristic curves.	20
A2. Watervliet Buttress for axial stress of 0.0.	21

	<u>Page</u>
A3. Watervliet Buttress for axial stress of 2.0.	22
A4. Watervliet Buttress for axial stress of 5.0.	23
A5. Watervliet Buttress for axial stress of 10.0.	24
A6. British Standard Buttress for axial stress of 0.0.	25
A7. British Standard Buttress for axial stress of 2.0.	26
A8. British Standard Buttress for axial stress of 5.0.	27
A9. British Standard Buttress for axial stress of 10.0.	28
A10. U.S. Standard Buttress from Heywood.	29
A11. FRG 120 mm from Heywood.	30
A12. Whitworth from Heywood.	31
A13. ISO Standard "V" cut and rolled from Heywood.	32
A14. Controlled root "V" for axial stress of 0.0.	33
A15. Controlled root "V" for axial stress of 2.0.	34
A16. Controlled root "V" for axial stress of 5.0.	35
A17. Controlled root "V" for axial stress of 10.0.	36
A18. 175 mm - 8 Inch block from Heywood.	37
A19. 175 mm - 8 Inch bushing from Heywood.	38
A20. 175 mm - 8 Inch tube from Heywood.	39

INTRODUCTION

The concept that stress or flow lines concentrate around various structural discontinuities is very old and has been the subject of many books and technical papers. It is convenient to express this concept in terms of a stress concentration factor (K) using the simple equation:

$$\sigma_{\max} = K \sigma_{\text{non}} .$$

Where K is a ratio between the maximum stress and some nominal stress, the single book, Stress Concentration Factors, by R. E. Peterson¹ is a compilation of the work included in some 378 references. The bulk of this work is contained on graphs which are plots of K vs. some geometry factor and most use a family of curves to show the effect of some other geometry factor. These plots provide both useful numeric information and a quick visual picture of the structural response.

The concept of stress concentration in screw threads is rather elusive and in fact there is little work done on stresses in threads. R. B. Heywood² published an empirical equation for the maximum fillet stress which was used in the work of Weigle, Lasselle and Purtell³ as a guide in trying to improve fatigue life of cannon breech rings.

¹Peterson, R. E., Stress Concentration Factors, John Wiley & Sons, New York, 1974.

²Heywood, R. B., "Tensile Fillet Stresses in Loaded Projections," Proceedings of the Institute of Mechanical Engineers, Vol. 160, p. 124, 1960.

³Weigle, Lasselle, and Purtell, "Experimental Behavior of Thread-Type Projections," Experimental Mechanics, May 1963.

Later this author demonstrated that the Heywood equation would give accurate numeric data when the boundary conditions were closely controlled.⁴

However, most work with screw threads seems to be done for specific cases such as the fine work of M. Hetinyi⁵ who investigated bolt shank and nut design in Witworth threaded bolts. This type of analysis using three dimensional photoelasticity was also used by W. F. Franz⁶ and J. D. Chalupnik.⁷ A further attempt at optimizing a thread form was done by R. L. Marino and W. F. Riley.⁸

In all of these works the calculated stress concentration factor is different for each thread in the system. It would seem that if the stress concentration factor is properly defined something should be a constant for all threads of a specific shape. In his original paper, Heywood demonstrated part of the problem. The stress in the fillet is the result of two factors. First, is the stress due to the load on the individual thread tooth and second, is the stress due to the general

⁴O'Hara, G. P., "Finite Element Analysis of Threaded Connections," Proceedings of the Fourth Army Symposium on Solid Mechanics, September 1974.

⁵Hetinyi, M., "The Distribution of Stress in Threaded Connections," Proceedings of SESA, Vol. 1, No. 1, 1943.

⁶Franz, W. F., "Three-Dimensional Photoelastic Stress Analysis of a Threaded Pipe Joint," Proceedings of SESA, Vol. 9, No. 2, pp. 185-194, 1952.

⁷Chalupnik, J. D., "Stress Concentration in Bolt Thread Roots," Experimental Mechanics, 1967.

⁸Marino, R. L., and Riley, W. F., "Optimizing Thread-Root Contours Using Photoelastic Methods," Experimental Mechanics, January 1964, p. 1.

stress field or the axial stress (σ_a) near the thread fillet. In this paper I will add effect due to friction and normalize all stresses to the average shear transfer rate (τ_R).

When the friction force and the force due to the "wedge" effect of the loaded flank of the thread are combined, a radial (normal) force is produced which can be averaged into the radial stress (σ_r). The fillet stress (σ_F) can be expressed as the sum of two functions.

$$\sigma_F/\tau_R = \bar{\sigma}_F = G_1(\alpha, \beta, \bar{R}, \theta, \bar{\sigma}_r) + G_2(\alpha, \beta, \bar{R}, \theta, \bar{\sigma}_a)$$

In the above equation the first function (G_1) is the relation between fillet stress and the load on the individual thread tooth. The second function (G_2) is the factor due to the general stress field. Alpha (α), beta (β), and \bar{R} are the thread geometry factors. The angle (θ) is in both functions because they do not maximize at the same position in the fillet. In this paper the shear transfer rate is defined as the net load supported by the thread divided by the area at the pitch line. The direction of the net load is parallel to the pitch line and in the analysis this component of the force will be unity. The radial stress ($\bar{\sigma}_r$) and axial stress ($\bar{\sigma}_a$) are normalized to the shear transfer rate.

The above discussion relates to a normal screw thread problem where only one flank of a particular thread contacts one flank of a mating thread. In some structures the relative displacement in the radial direction across the threaded connection is such that the radial gap in the threads is closed and both flanks of each thread carry load. Under these conditions the radial component of the loads add together

to produce high negative or compressive radial stress across the joint. The axial loads oppose each other and the pressure on the primary flank must become very high to overcome the secondary flank load. This is not a common condition; however, it may become very important in the cannon breech-to-tube connection.

THREAD GEOMETRY

The thread geometry parameters are shown in Figure 1 and in this report all linear dimensions will be normalized to pitch (P). The primary geometry parameters are the primary flank angle (α), the secondary flank angle (β) and the root radius \bar{R} . These, in conjunction with the pitch space (Pl), define the basic thread geometry. Other factors are required to insure a practical thread which will fit together. The addendum (AD) and dedendum (DD) dimensions sum to the total height (HT). The tip radius (RT) eliminates a sharp corner and helps to support the bearing surface. The root flat (FLAT) is often used to make up for the root radius tolerance. The bearing height (Z) is used to calculate the average bearing stress and the shear length (S) is used to calculate the maximum shear-out failure load.

This complicated system is simplified by the fact that we must deal with a small set of standard thread forms. In this report detailed analysis has been done on the British Standard Buttress thread and Heywood analysis has also been done on the controlled root bolt thread or "J" thread and the Watervliet Arsenal Buttress used on cannon breeches. The nominal dimensions for these threads are shown in Table I.

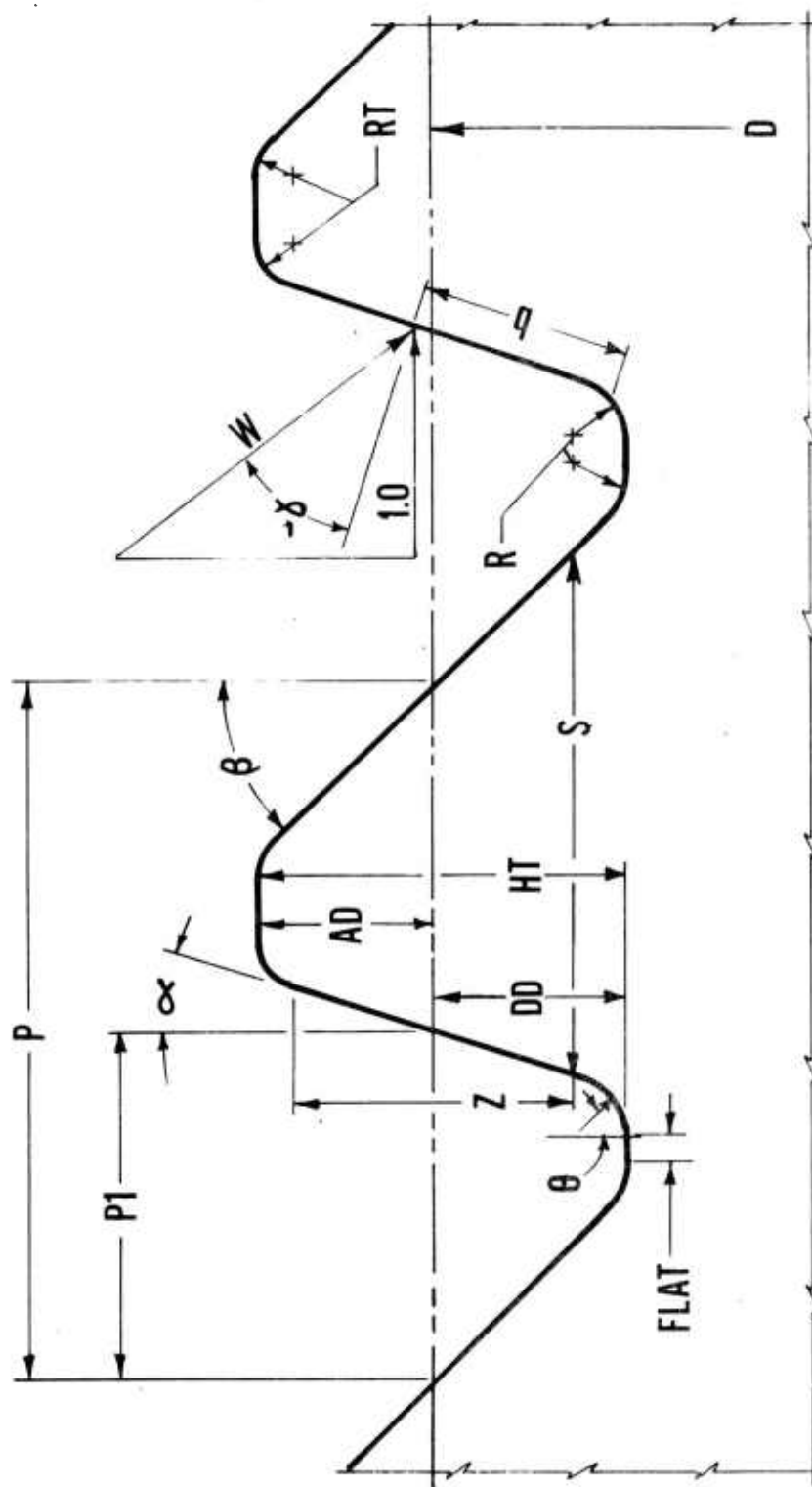


Figure 1. THREAD GEOMETRY AND LOAD PARAMETERS

TABLE I. THREAD GEOMETRY DEFINITION

	British Buttress	Watervliet Buttress	30 "V" (Rolled)
α	7°	20°	30°
β	45°	45°	30°
\bar{R}	0.1205	0.1333	0.1804
P1	0.500	0.5276	0.500
HT	0.5059	0.4787	0.6077
RT	0.00	0.0480	0.1083
FLAT	0.0	0.0	0.0

LOADING PARAMETERS

The Heywood load parameters are also shown in Figure 1. They are a point force (W) applied at some position (b) in the loaded flank with a friction angle (γ). This scheme can be repeated many times on the loaded flank to produce some load distribution curve. The following loading assumptions are made:

1. The total load vector parallel to the datum line is unity.
2. The load distribution is uniform.
3. Friction does not vary along the flank.

The first assumption given allows the normalization of stresses to shear transfer rate and the other two establish a simple loading case.

Under conditions of high radial compressive load, it is possible for threads to be pushed together until both flanks contact on the thread and the radial stress become a function of the flank angle α and the friction angle γ :

$$\bar{\sigma}_r = \tan (\alpha - \gamma)$$

Note that friction becomes a signed variable depending on the relative displacement of the two components of the structure.

In the above discussion the general field or axial stress is assumed to be zero. In the NASTRAN finite element analysis the axial stress was simulated by the use of a constraint subcase in which the relative axial displacement between the two radial boundaries was fixed by the use of scalar points and multipoint constraint equations. The radial displacements on these planes were made equal for congruent points. The radial displacement of the inner axial boundary was set equal to the Poisson contraction of a solid bar.

HEYWOOD ANALYSIS

The Heywood equation is shown in Figure 2. This is a semi-empirical equation that was fit to a large body of photoelastic data. It calculates maximum fillet stress for a point load on the primary flank of a thread using a specific friction angle. In order to simulate a uniform load distribution, the results are averaged for seven different "b" values evenly distributed over the flank. The process has been programmed into a program called HEY40. The calculations have been done for many standard thread forms, and the three

$$\sigma_F = \left[1.0 + 0.26 \left(\frac{e}{R} \right)^{0.7} \right] \left[\frac{1.5a}{e^2} + \sqrt{\frac{0.36}{be}} \left(1.0 + \frac{1}{4} \sin \gamma \right) \right] \frac{W}{T}$$

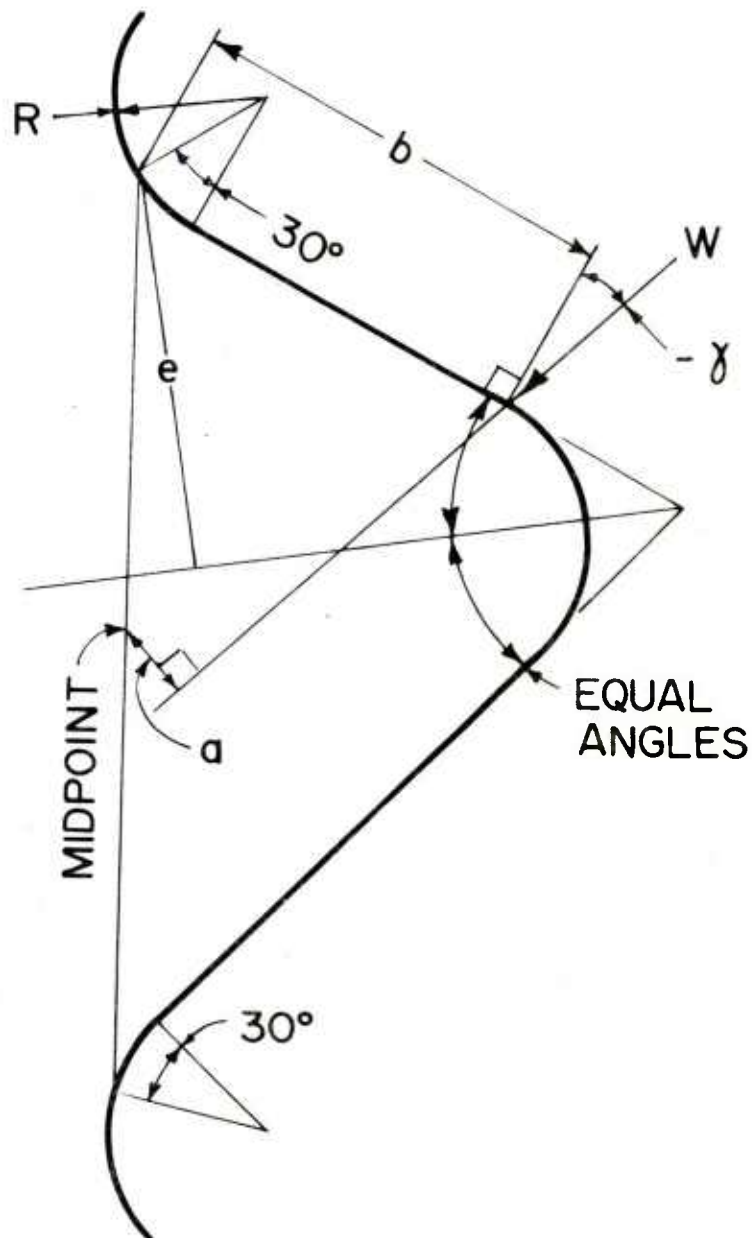


Figure 2. **HEYWOOD'S EQUATION**

THREAD CHARACTERISTIC FROM
HEYWOOD ANALYSIS FOR:

- ① = BRITISH STANDARD BUTTRESS
- ② = WATERVLIIET BUTTRESS
- ③ = CONTROLLED ROOT "V"

$$\bar{\sigma}_a = 0.0$$

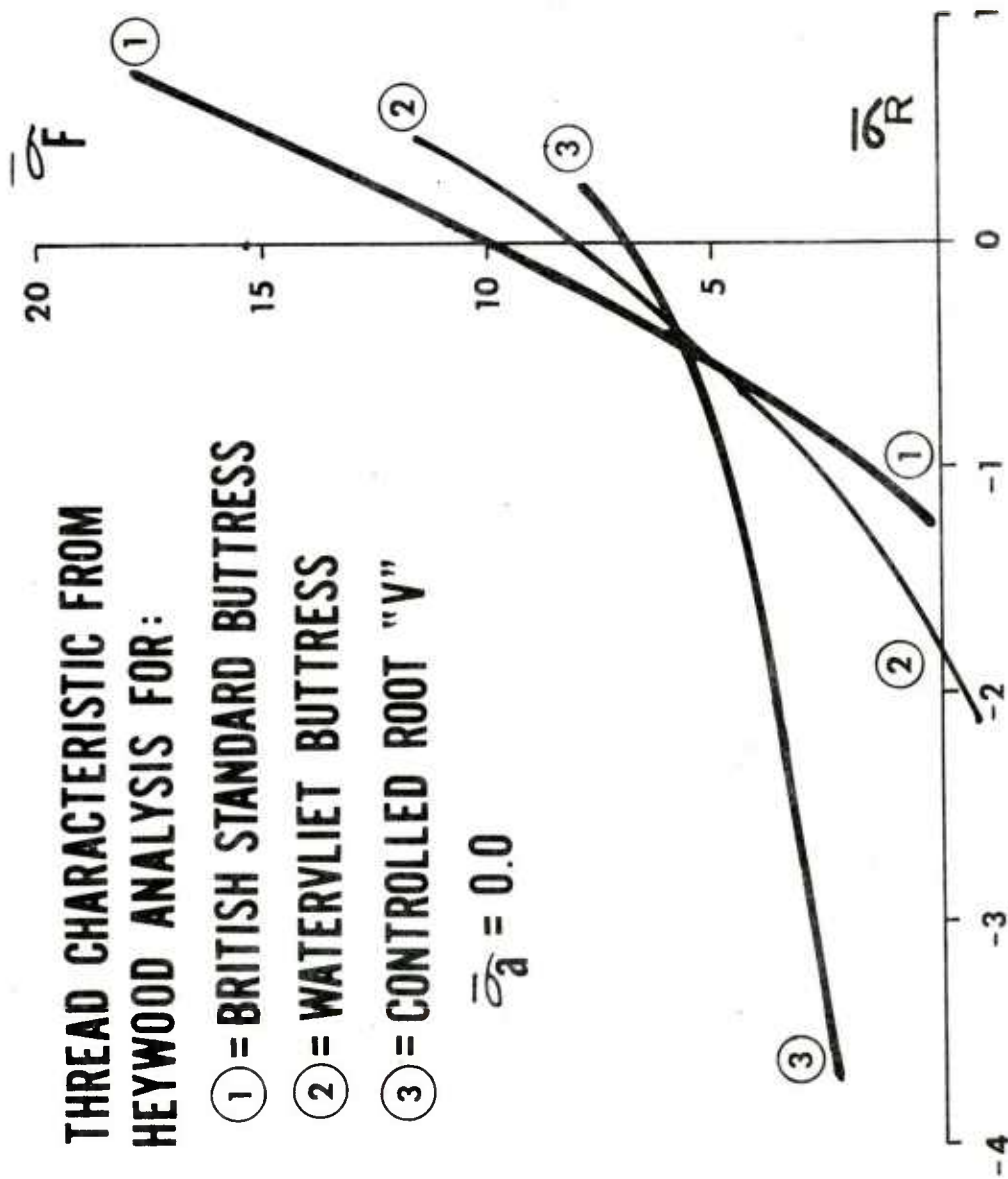


Figure 3.

reported in Figure 3 have been defined in Table I. This plot of fillet stresses plotted against radial stress will be referred to as the "thread characteristic curve". This curve covers a friction angle range of -45° to 45° or a coefficient of friction range of -1.0 to 1.0.

In Heywood's photoelastic experiments he was careful to transfer the load supported by the threads profiled in a shear mode to make the axial stress as small as possible. This process limited his equation to the case where axial stress is equal to zero.

NASTRAN FINITE ELEMENT ANALYSIS

The finite element work was done for three reasons: (1) to verify the Heywood analysis; (2) to examine the two-flank problem; and (3) to include a finite axial stress. The grid for the British Standard Buttress is shown in Figure 4. It contains 216 triangular ring elements (CTRIARG) and 133 grid points. The run required five basic loading subcases plus fourteen subcase combinations for each value of axial stress. These fourteen subcases cover both 1-flank and 2-flank contact over a range coefficient of friction of -1.0 to 1.0 in increments of 0.25.

The grid was generated using IGFES⁹ and following that, force sets were calculated to apply uniform pressure and uniform shear loads on both flanks of the thread and a displacement was calculated for a nominal 1.0 psi axial load on the grid. Two different constraint

⁹Lorensen, W. E., "Interactive Graphic Support for NASTRAN," Sixth NASTRAN User's Colloquium, NASA Conference Publication 2018, October 1977.

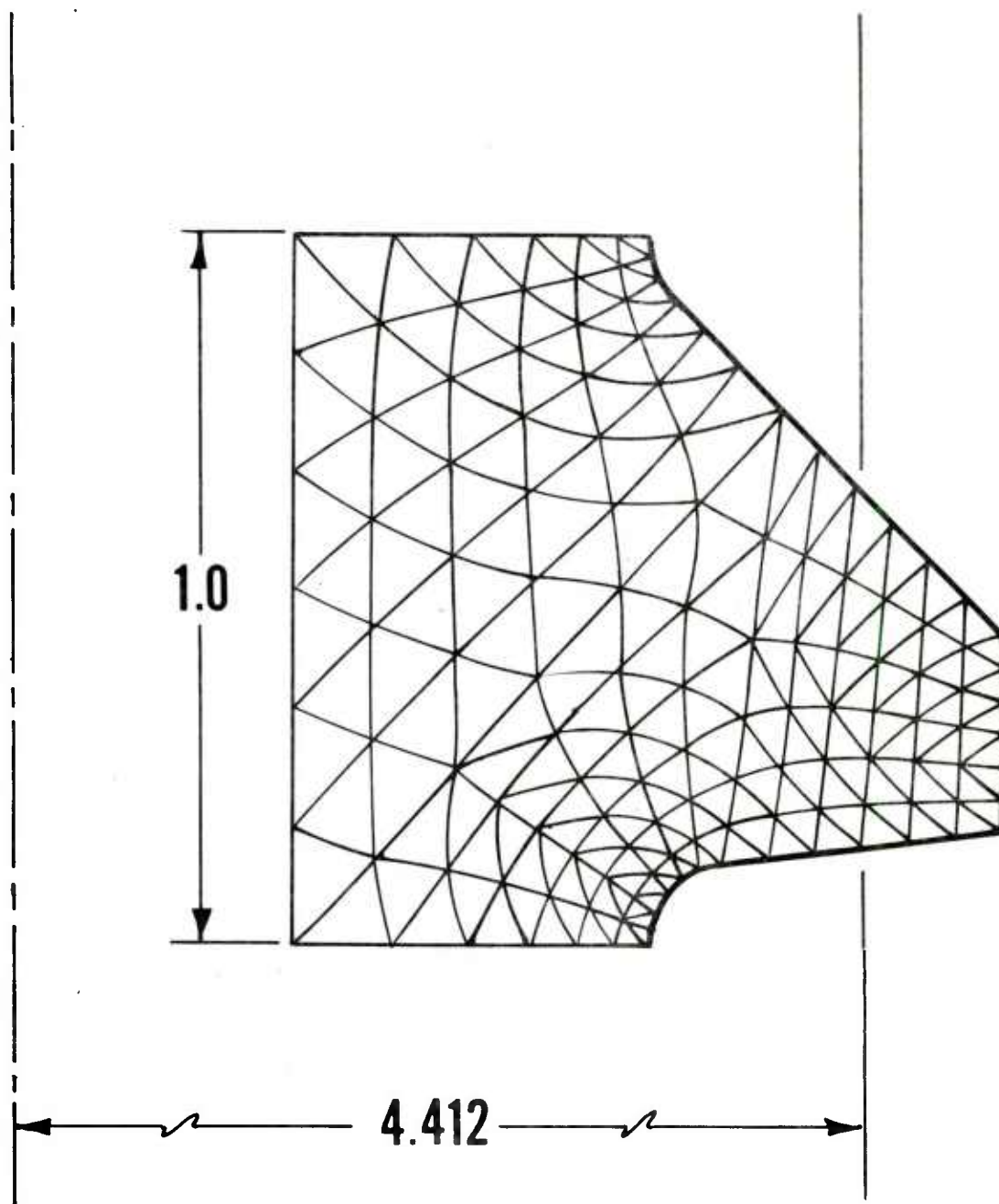


Figure 4. NASTRAN GRID

conditions were required to complete the boundary conditions for a single thread taken from a long series of threads. For loads on the thread the inner boundary points were fixed in both radial and axial directions and similar points on the two radial boundaries were constrained to equal displacements. In this way the net load was taken out as shear load on the inner axial boundary and the multipoint constraint equations replaced adjoining material. For the axial load condition the inner axial boundary was constrained to the Poisson displacement in the radial direction and left free in the axial direction. The two radial boundaries were given fixed relative axial displacements and the radial displacement was made equal for similar grid points. This condition was set to simulate a far removed axial loading.

Because the basic loads were all for a 1.0 psi uniform applied pressure or shear and the results were desired for a 1.0 psi shear transfer rate (calculated at the datum line), it became necessary to calculate the correct Subcase Sequence Coefficients for fourteen subcases for each of four axial stress values (or 56 sets). Therefore a small program was generated to supply all necessary SUBCOM, SUBSEQ and LABEL cards for that portion of the case control deck.

Uniform increments of 0.25 in coefficient were used from -1.0 to 1.0. If the friction was zero or less, a similar subcase combination was generated along with one where both flanks were loaded and the second radial stress was 1.0 greater than the initial.

The axial load subcase produced the conventional fillet stress concentration factor of $K = 2.89$. This maximum stress was in an element at the bottom of the fillet where θ is approaching 0° . In the cases where the load is applied to the thread the exact position of the stress maximum is about 45° up from the bottom of the fillet. Data is reported here for two cases of axial stress. Zero axial stress is shown in Figure 5 and axial stress of 2.0 is shown in Figure 6. These plots are a set of six lines with the single contact curve at the right. Starting at that curve is a family of five lines going to the left which represent two flank contacts at different values of friction from 0 to -1.0.

DISCUSSION

The first thing to note is that there is excellent agreement between Heywood and NASTRAN over most of the range of the plots for the one case in question. Because of this, the Heywood relation can be used to evaluate different thread forms. The finite element method has allowed the expansion of the basic plot to the 2-flank contact problem and the addition of the axial stress.

There are several important points that are demonstrated by this work. Note that a small change in friction can produce a large fillet stress variation in all three threads reported in the Heywood analysis. Negative friction angles can produce marked reductions in thread fillet stress. This effect was noted several years ago in an unpublished three dimensional photoelastic study where the model was overloaded and

FIGURE 5.
THREAD CHARACTERISTIC CURVE
 BRITISH STANDARD BUTTRESS
 $\bar{\sigma}_a = 0.0$

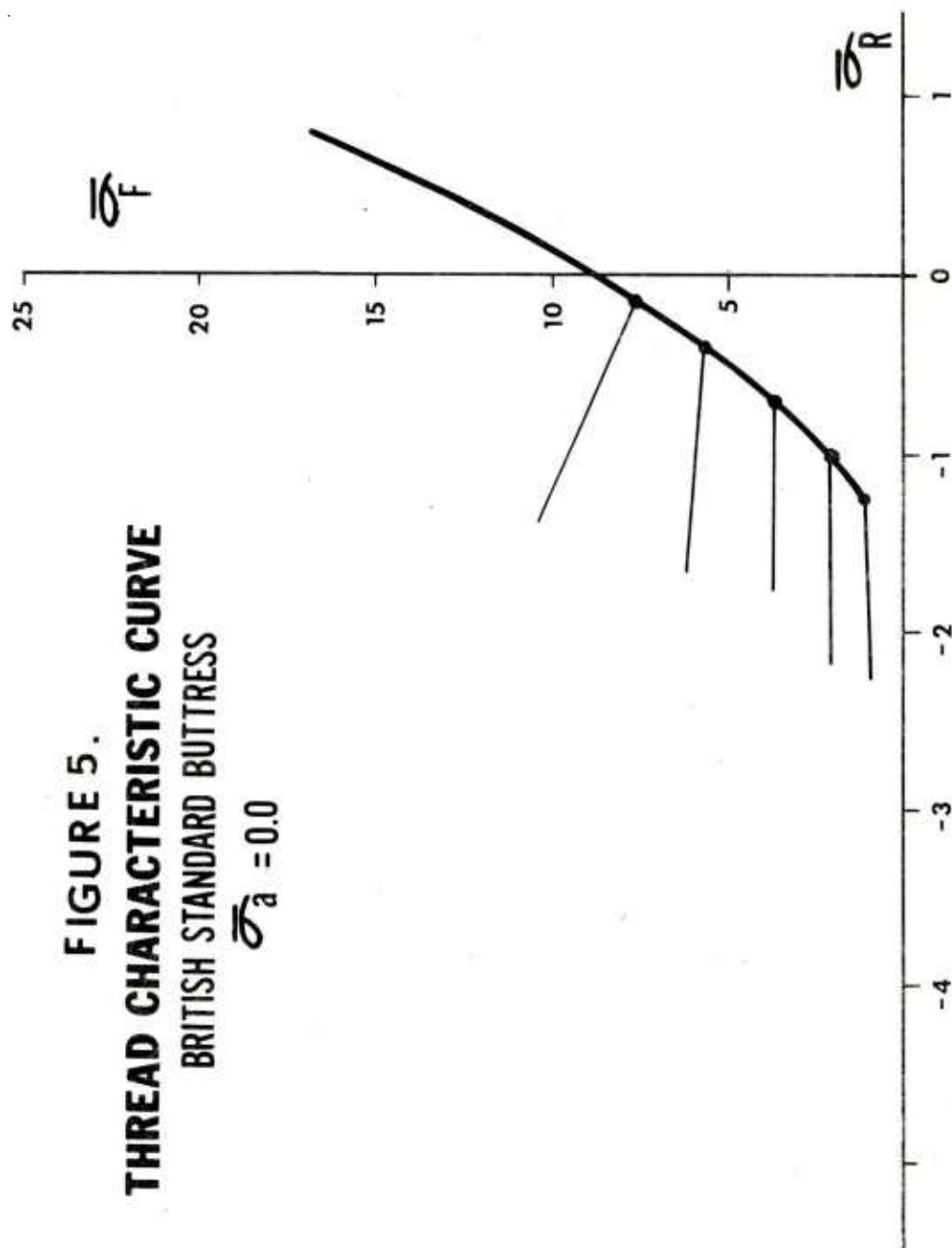
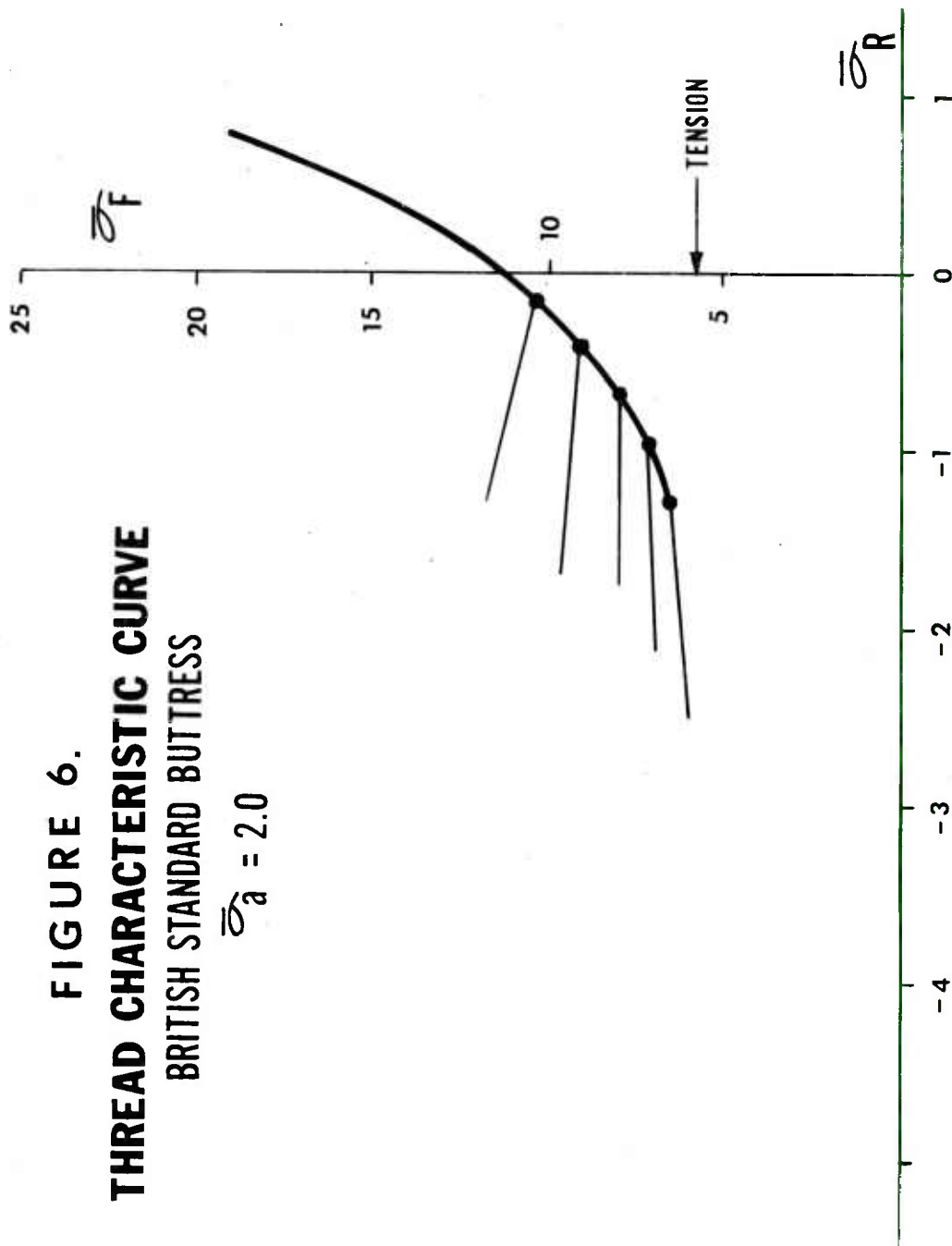


FIGURE 6.
THREAD CHARACTERISTIC CURVE
BRITISH STANDARD BUTTRESS

$$\sigma_a = 2.0$$



the threads were forced to a high negative radial stress. In this case the fillet stresses were very low and the experiment was repeated. This author suspects that friction variation may be responsible for much of the scatter in bolt-fatigue data.

This work was initiated because of the necessity of analyzing a structure with a long threaded connection using many small threads. In this case the modeling of each thread would require an excessively large data deck. Therefore, the threads were handled as a conventional contact problem where friction could take on any value and limits were applied to the radial stress. In the solution the contact surface was placed on the datum line of the threads and one or two teeth were replaced by one element space. Shear transfer rates could then be estimated from the shear stress data near the contact surface along with radial and axial stress. The fillet stresses were estimated for use in fracture mechanics analysis.

CONCLUSION

A stress concentration approach to the thread fillet stress problem has been defined using the shear transfer rate as the fundamental quantity. This stress concentration is plotted for a fixed geometry in a stress vs. stress plot where the stress concentration is a function of the applied radial stress. This process can be repeated for several values of the applied axial load. The effects of axial stress and applied thread loads seem to be of equal importance and accurate results require the analysis of both factors.

REFERENCES

1. Peterson, R. E., Stress Concentration Factors, John Wiley & Sons, New York, 1974.
2. Heywood, R. B., "Tensile Fillet Stresses in Loaded Projections," Proceedings of the Institute of Mechanical Engineers, Vol. 160, p. 124, 1960.
3. Weigle, Lasselle and Purtell, "Experimental Behavior of Thread-Type Projections," Experimental Mechanics, May 1963.
4. O'Hara, G. P., "Finite Element Analysis of Threaded Connections," Proceedings of the Fourth Army Symposium on Solid Mechanics, September 1974.
5. Hetinyi, M., "The Distribution of Stress in Threaded Connections," Proceedings of SESA, Vol. 1, No. 1, 1943.
6. Franz, W. F., "Three-Dimensional Photoelastic Stress Analysis of a Threaded Pipe Joint," Proceedings of SESA, Vol. 9, No. 2, pp. 185-194, 1952.
7. Chalupnik, J. D., "Stress Concentration in Bolt Thread Roots," Experimental Mechanics, 1967.
8. Marino, R. L., and Riley, W. F., "Optimizing Thread-Root Contours Using Photoelastic Methods," Experimental Mechanics, January 1964, p. 1.
9. Lorensen, W. E., "Interactive Graphic Support for NASTRAN," Sixth NASTRAN User's Colloquium, NASA Conference Publication 2018, October 1977.

APPENDIX A

This appendix was written to provide an expanded data base for the application of the thread characteristic plot concept. The curves quoted are from one of two sources, finite element analyses using the NASTRAN code or the solution of Heywood's equation using a small program called HEY40. The basic curves calculated from Heywood use an average of seven distributed loads at each data point. The NASTRAN run use a constant pressure or shear type of loading. These plots also add the two face contact condition and provide a separate plot for axial stresses of 0.0, 2.0, 5.0, and 10.0 times the shear transfer rate.

Table I shows the geometry parameters for all the thread forms in question. The definition of these can be taken from Figure 1 of the main body of the report.

Figure A1 in the Appendix is a plot of the conventional tensile stress concentration factor vs. nondimensional root radius (\bar{R}). This is the result of NASTRAN analysis of the threads in the Appendix and other thread like projections. It appears that this tensile stress concentration provides the minimum stress value to which stress due to Heywood type loads are added to provide the maximum stress in the fillet.

TABLE A1. THREAD GEOMETRY PARAMETERS

Thread	α	β	\bar{R}	\bar{RT}	Z	S
Watervliet Buttress	20	45	.133	.048	.395	.731
British Standard Buttress	7	45	.121	.0	.400	.724
U.S. Standard Buttress	7	45	.071	.0	.600	.837
FRG 120 mm*	3	45	.105	.040	.362	.679
Whitworth	27.5	27.5	.137	.137	.493	.756
ISO Standard 'V' (cut)	30	30	.144	.0	.542	.751
ISO Standard 'V' (rolled)	30	30	.144	.108	.488	.751
Controlled Root Symbol UNJ	30	30	.180	.108	.478	.740
175 mm - 8 Inch Block	35	35	.120	.182	.355	.803
175 mm - 8 Inch Bushing	15	37.15	.136	.0	.451	.725
175 mm - 8 Inch** Tube	14.5 14.5	14.5 14.5	.027 .013	.040 .040	.240 .250	.580 .585

*This form has a root flat of .072.

**A specific case of a Stub Acme Modified Form 2.

STRESS CONCENTRATION VS. ROOT RADIUS

FROM NASTRAN SOLUTIONS OF
THREADS AND THREAD-LIKE
LUGS.

- K_T
- O = SEMI-CIRCULAR NOTCH
 - = SPECIAL LUG SYSTEM
 - △ = THREADS

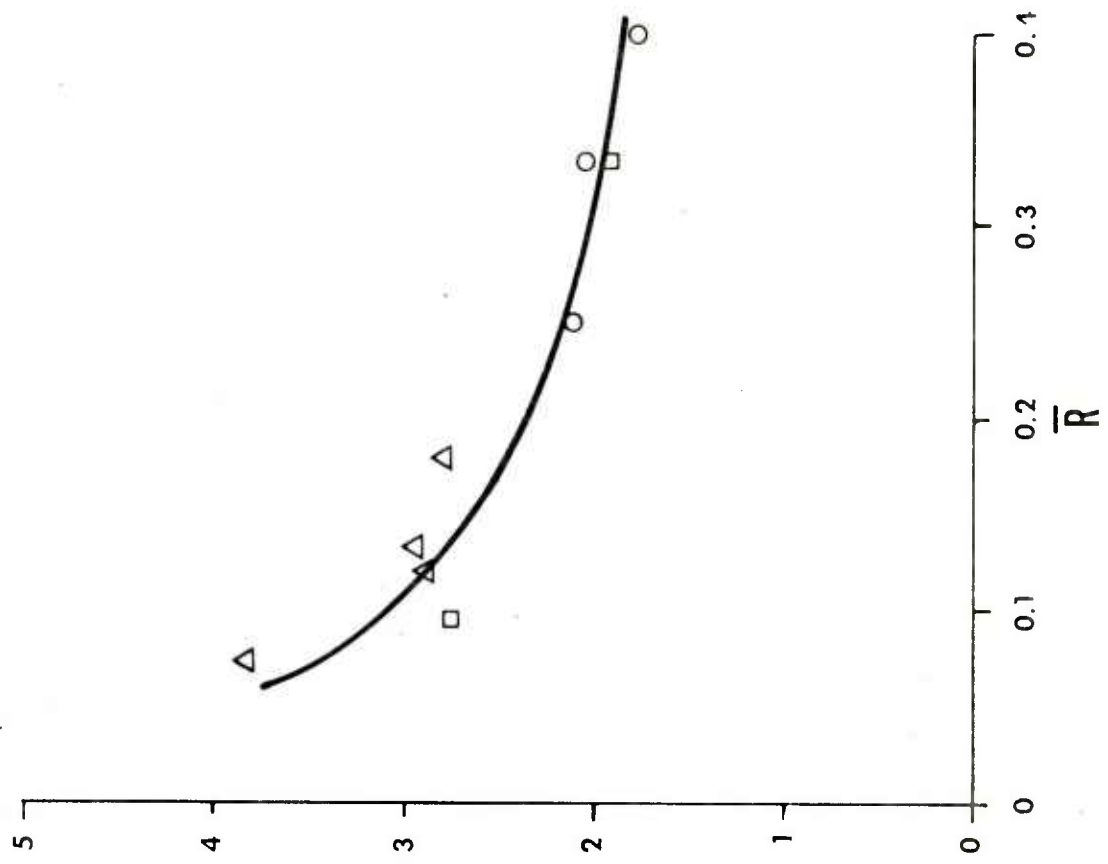


Figure A1. Axial stress concentration thread characteristic curves.

THREAD CHARACTERISTIC CURVE

WATERVLIET BUTTRESS

FINITE ELEMENT ANALYSIS

HEYWOOD'S EQUATION

$$\bar{\sigma}_a = 0.0$$

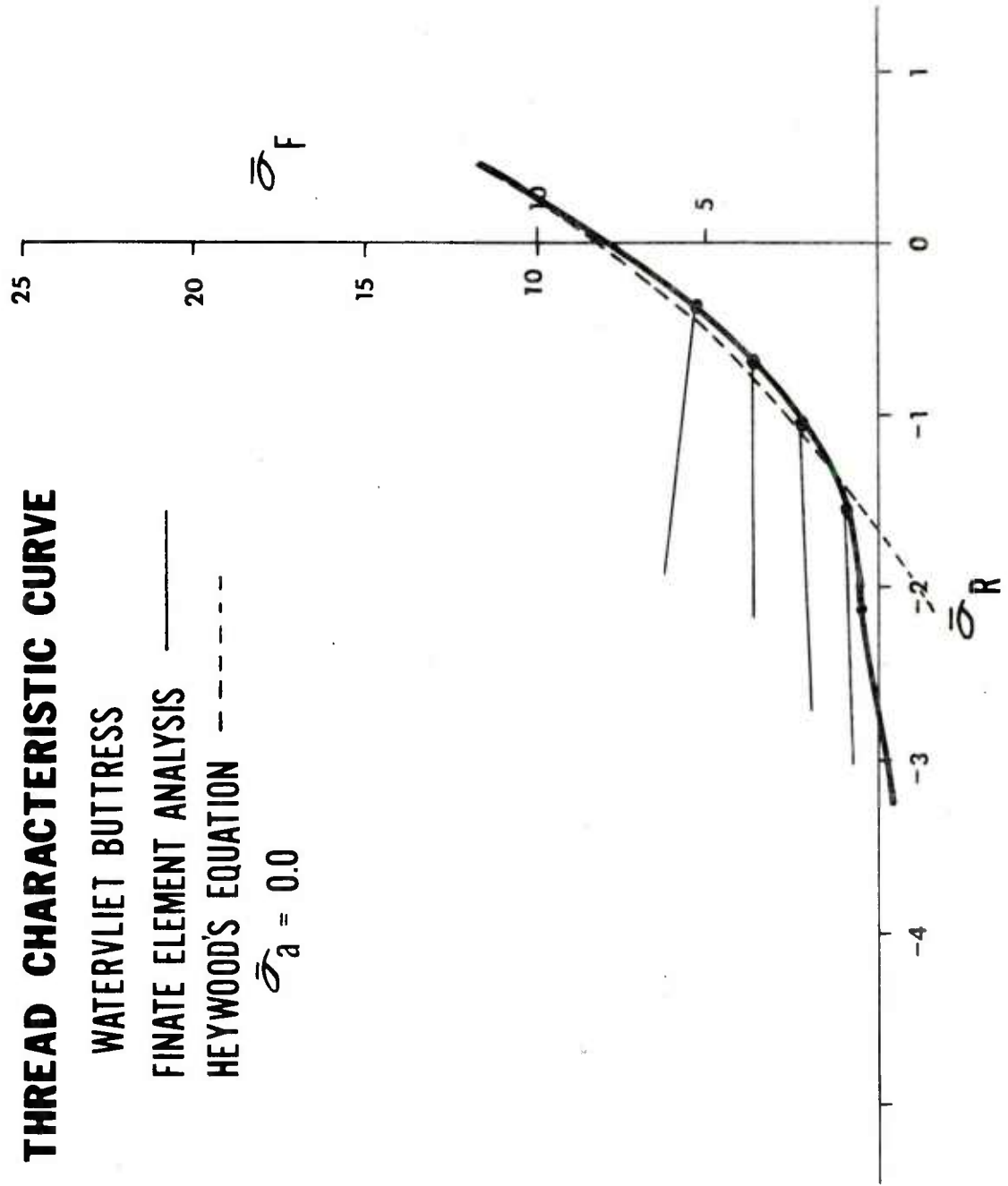


Figure A2. Watervliet Buttress for axial stress of 0.0.

THREAD CHARACTERISTIC CURVE

WATERVLIIET BUTTRESS

FINITE ELEMENT ANALYSIS

$$\bar{\sigma}_a = 2.0$$

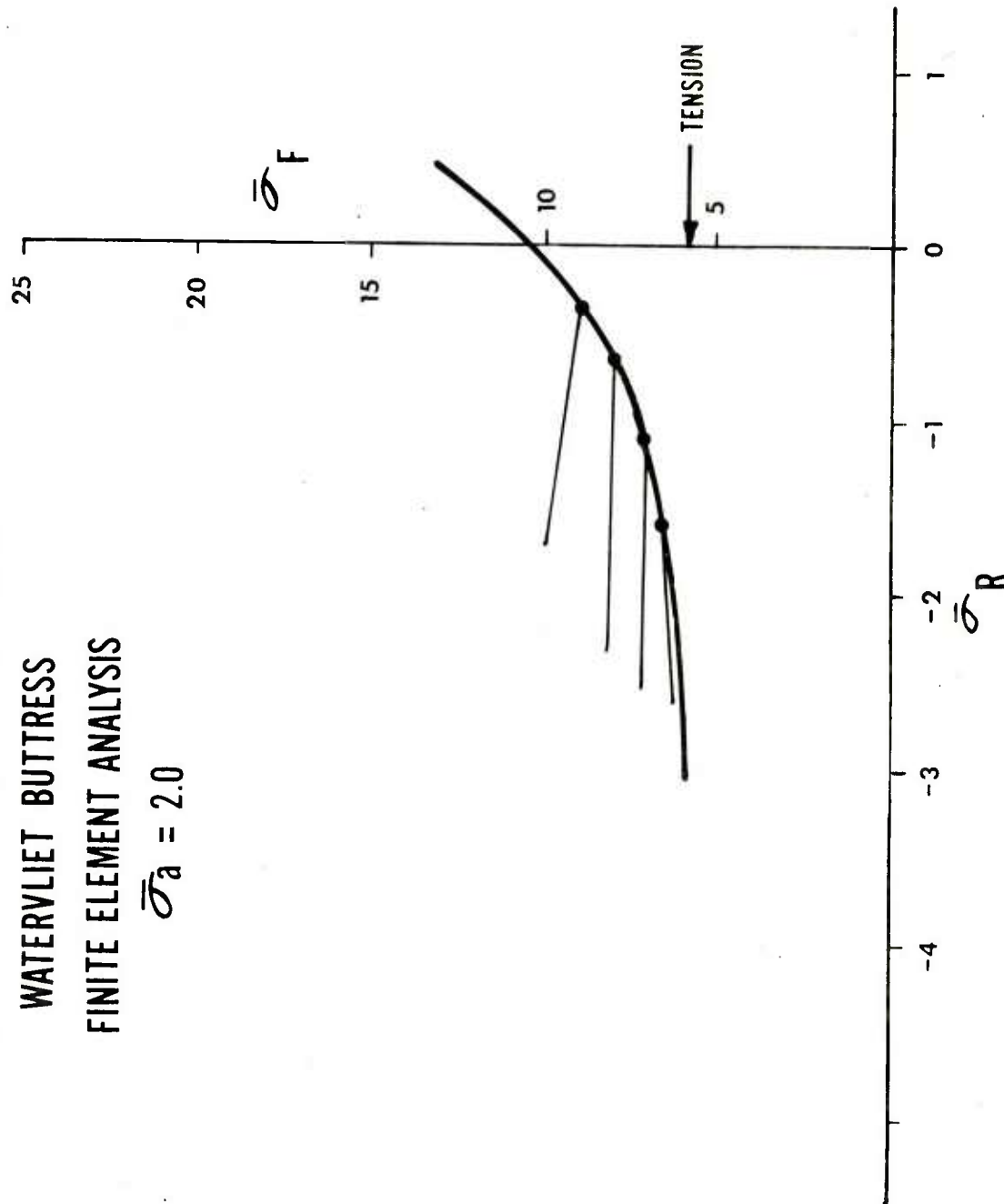


Figure A3. Watervliet Buttress for axial stress of 2.0.

THREAD CHARACTERISTIC CURVE

WATERVLIIET BUTTRESS
FINITE ELEMENT ANALYSIS

$$\bar{\sigma}_a = 5.0$$

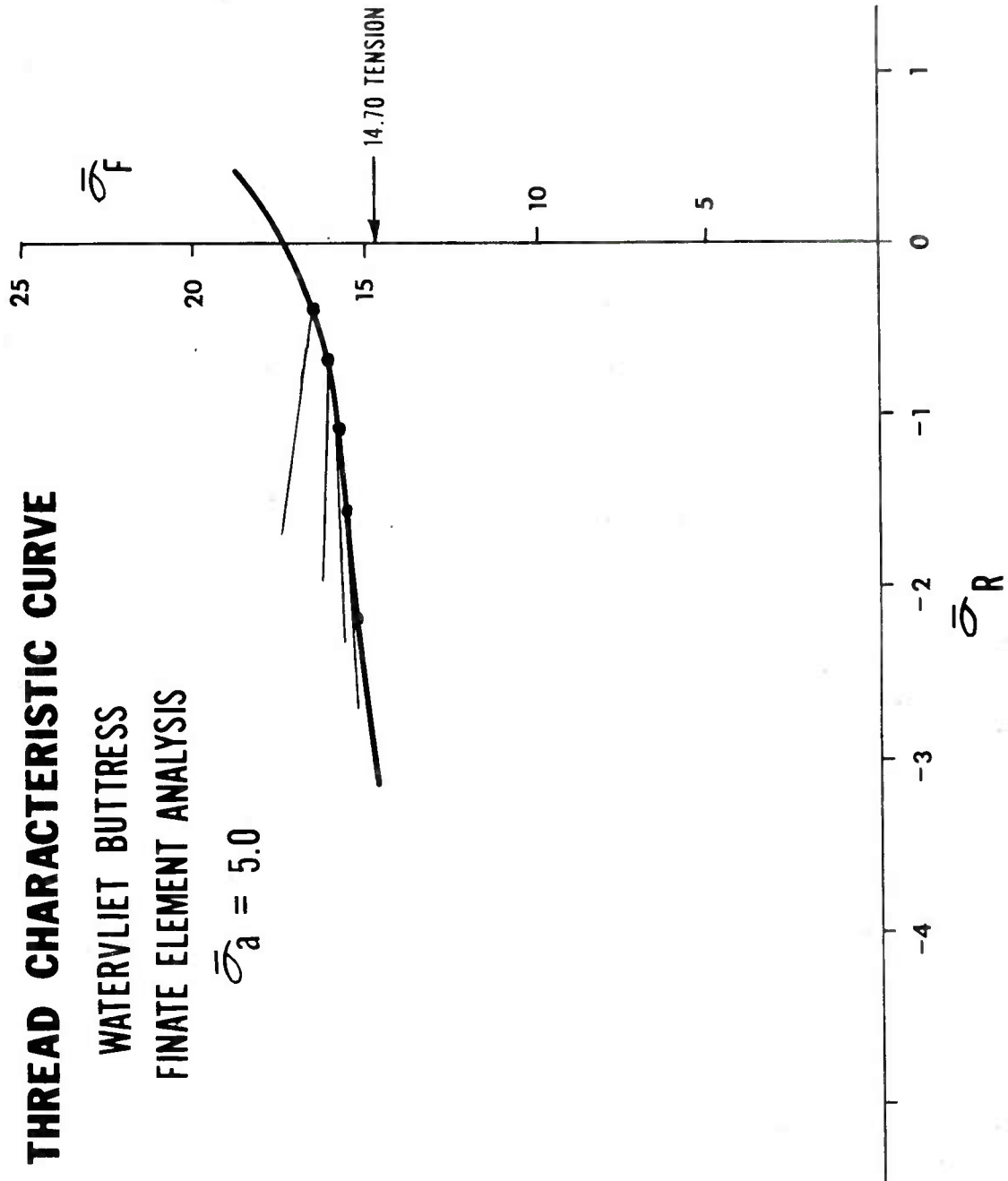


Figure A4. Watervliet Buttress for axial stress of 5.0.

THREAD CHARACTERISTIC CURVE

WATERVLIET BUTTRESS

FINITE ELEMENT ANALYSIS

$$\sigma_a = 10.0$$

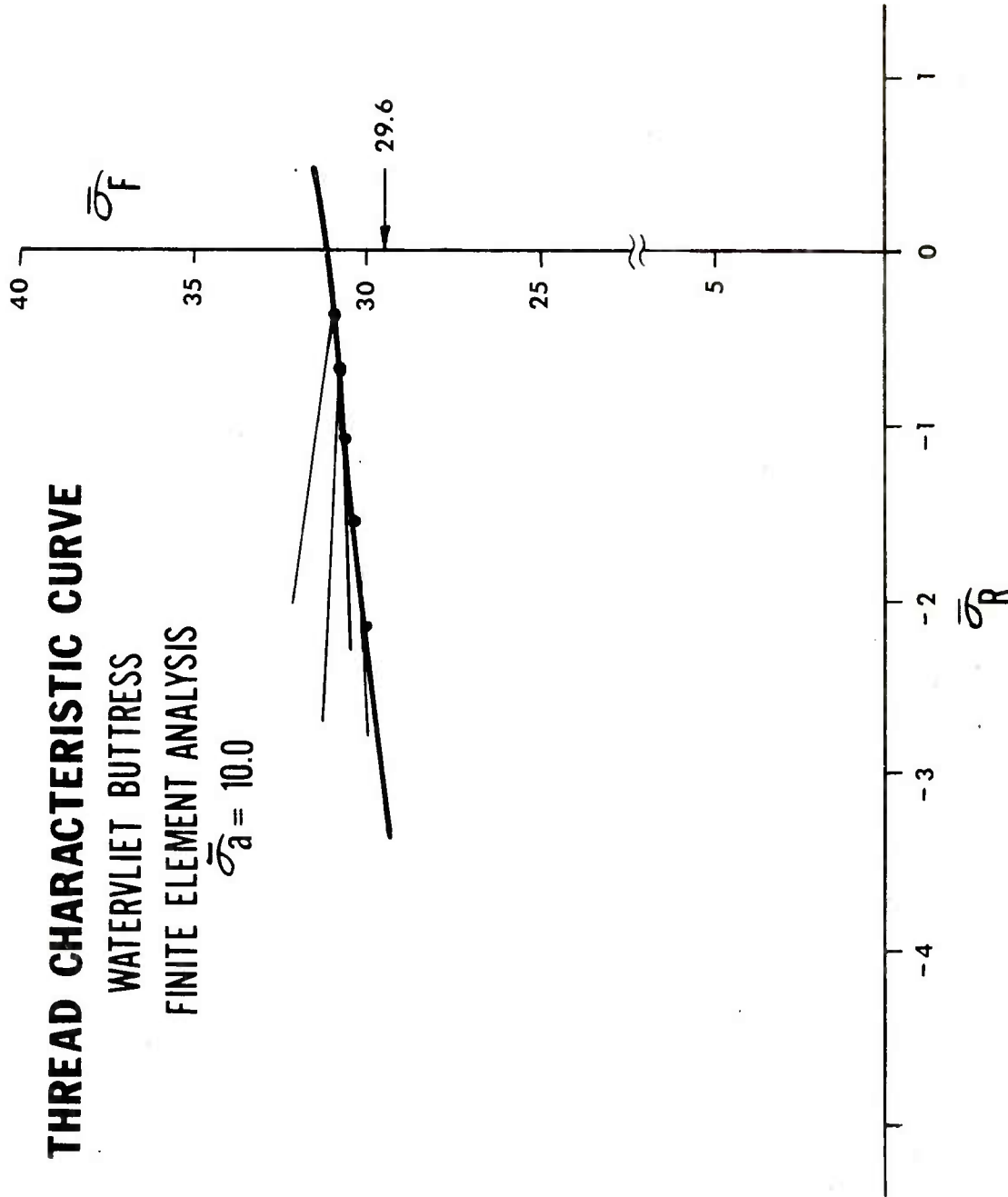


Figure A5. Watervliet Buttress for axial stress of 10.0.

THREAD CHARACTERISTIC CURVE

BRITISH STANDARD BUTTRESS

FINITE ELEMENT ANALYSIS —

HEYWOOD'S EQUATION ---

$$\sigma_a = 0.0$$

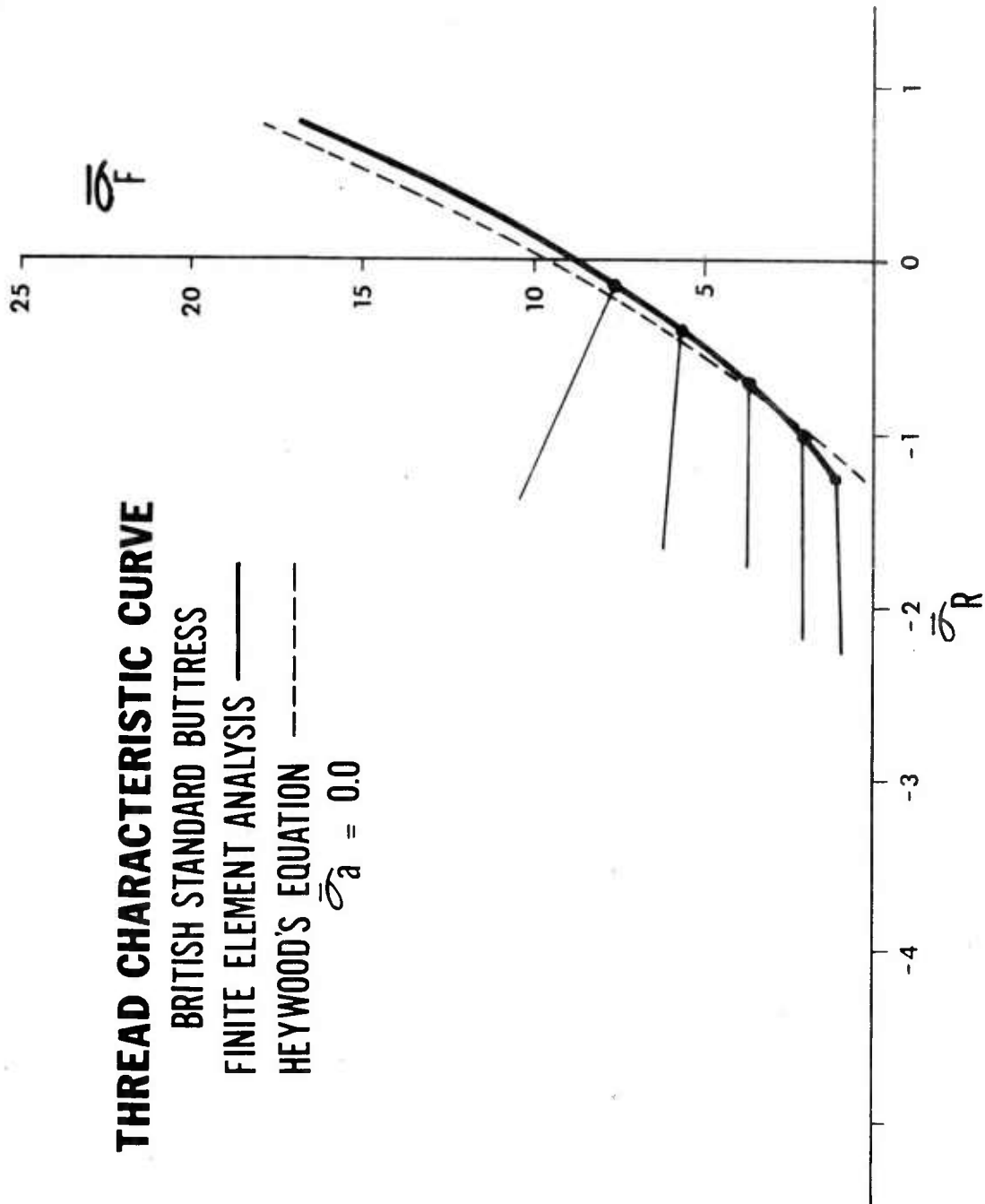


Figure A6. British Standard Buttress for axial stress of 0.0.

THREAD CHARACTERISTIC CURVE **BRITISH STANDARD BUTTRESS** **FINITE ELEMENT ANALYSIS**

$$\bar{\sigma}_a = 2.0$$

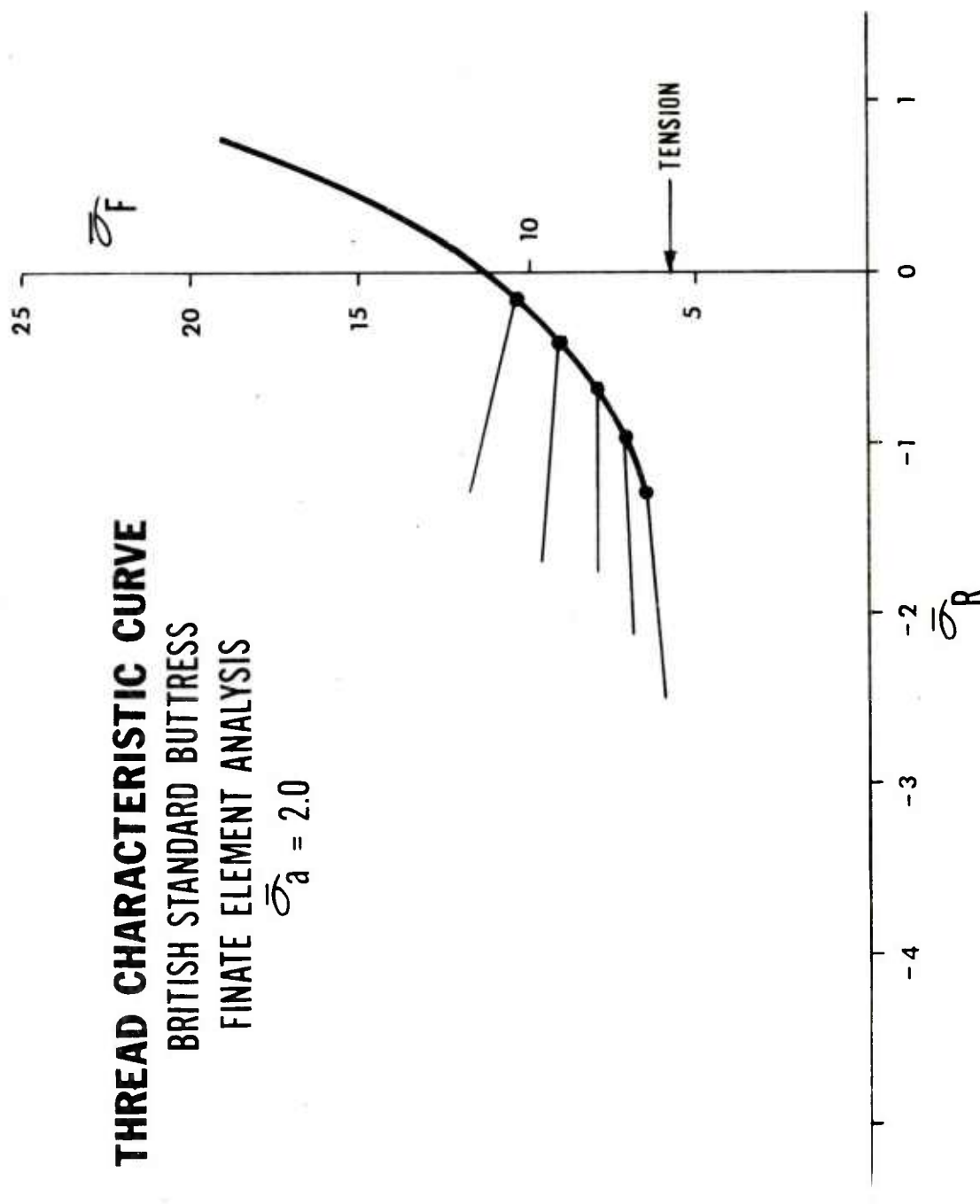


Figure A7. British Standard Buttress for axial stress of 2.0.

THREAD CHARACTERISTIC CURVE **BRITISH STANDARD BUTTRESS** **FINITE ELEMENT ANALYSIS**

$$\bar{\sigma}_a = 5.0$$

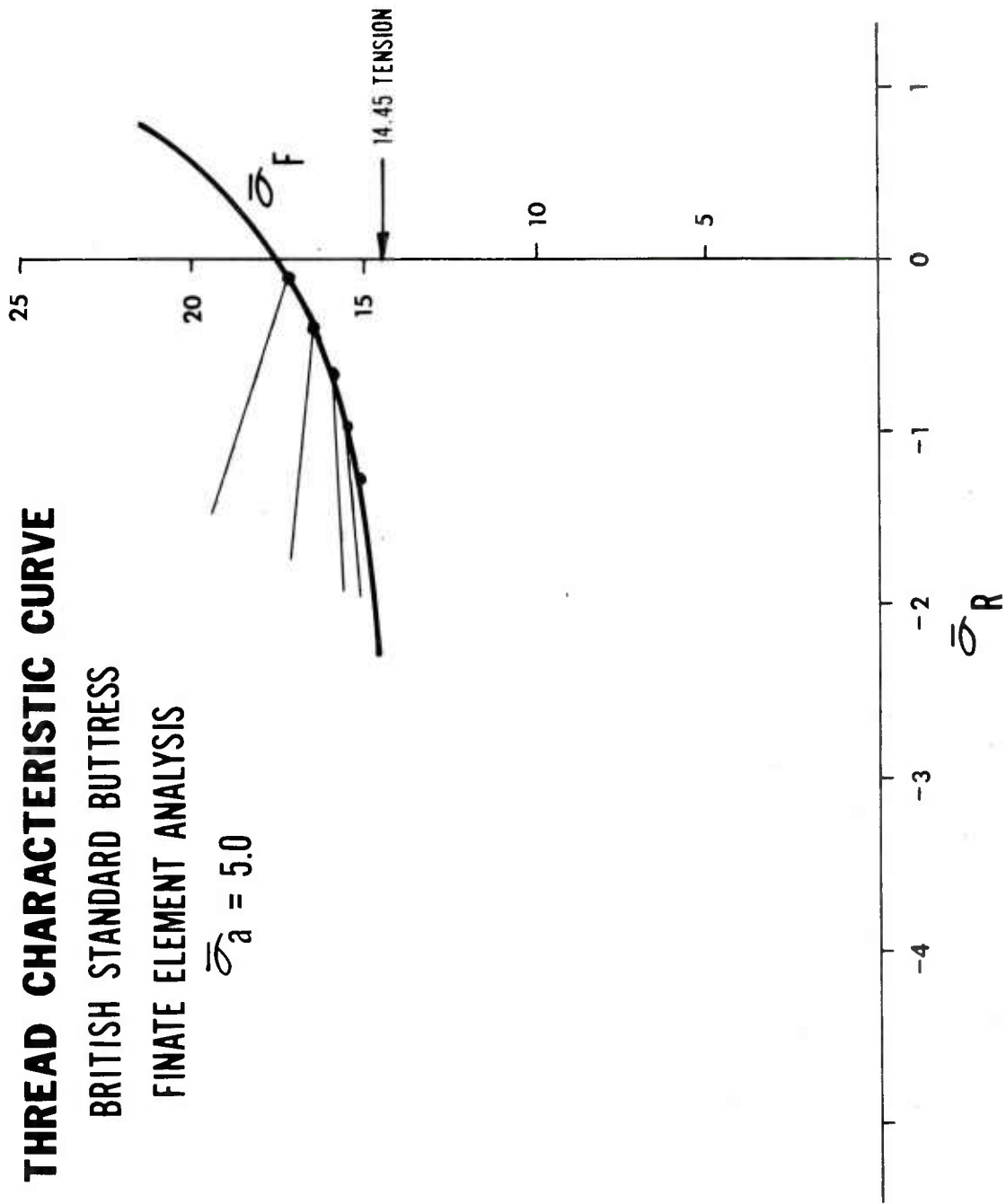


Figure A8. British Standard Buttress for axial stress of 5.0.

THREAD CHARACTERISTIC CURVE

BRITISH STANDARD BUTTRESS

FINITE ELEMENT ANALYSIS

$$\bar{\sigma}_a = 10.0$$

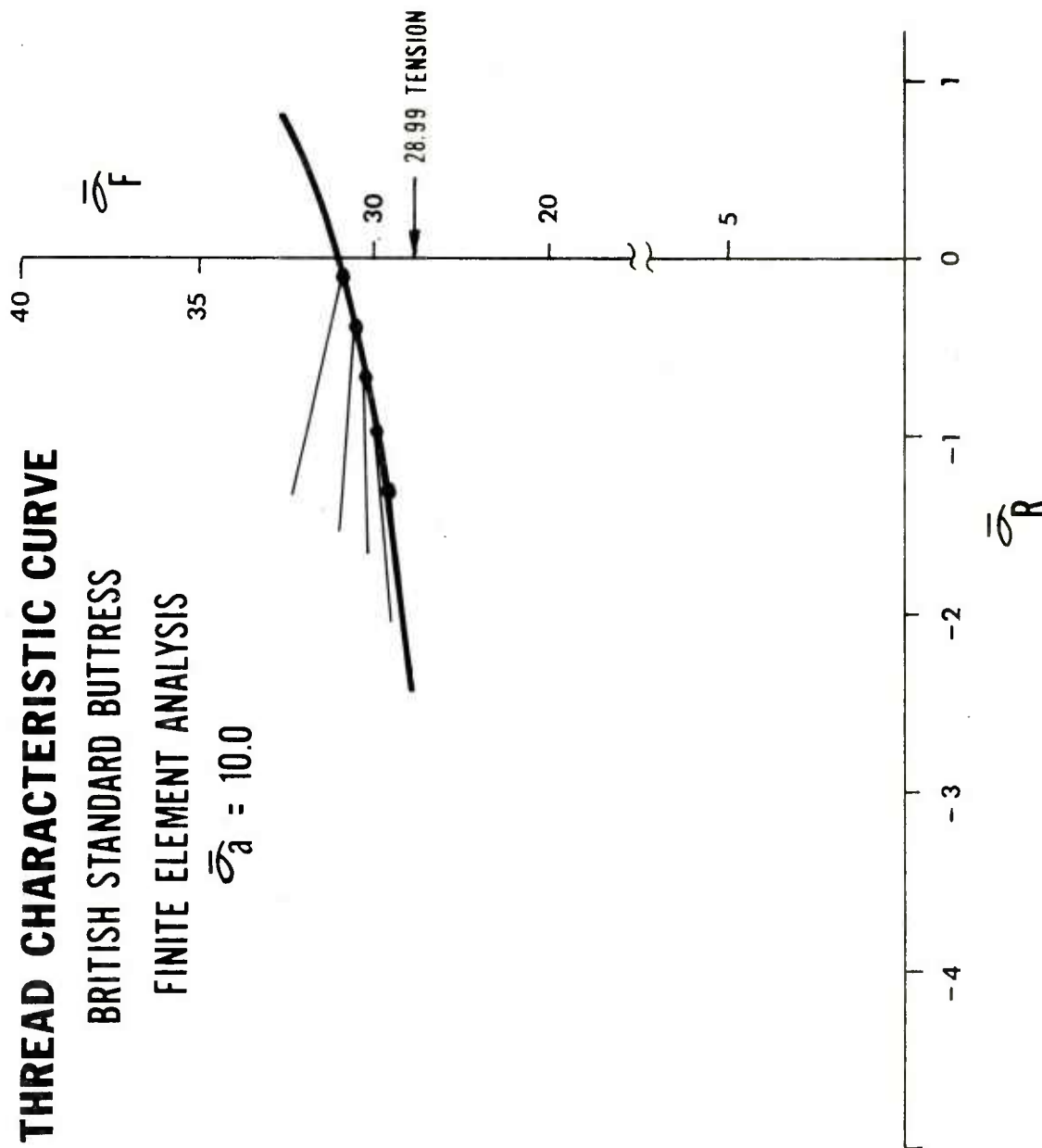


Figure A9. British Standard Buttress for axial stress of 10.0.

U.S. STANDARD BUTTRESS

7 - 45 - 0.071

HEYWOOD

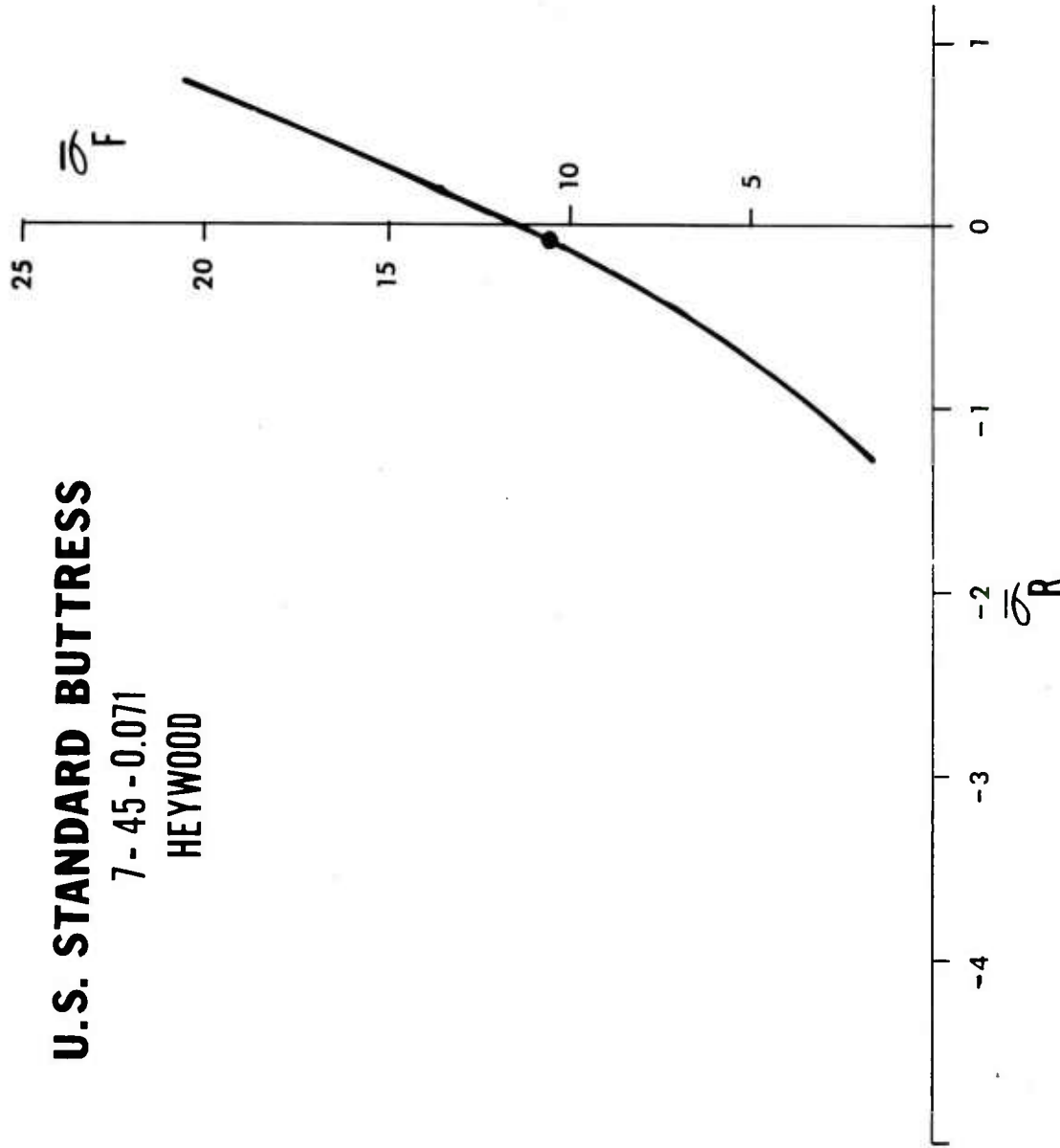


Figure A10. U.S. Standard Buttress from Heywood.

F.R.G. 120 MM
3 - 45 - 0.125
HEYWOOD

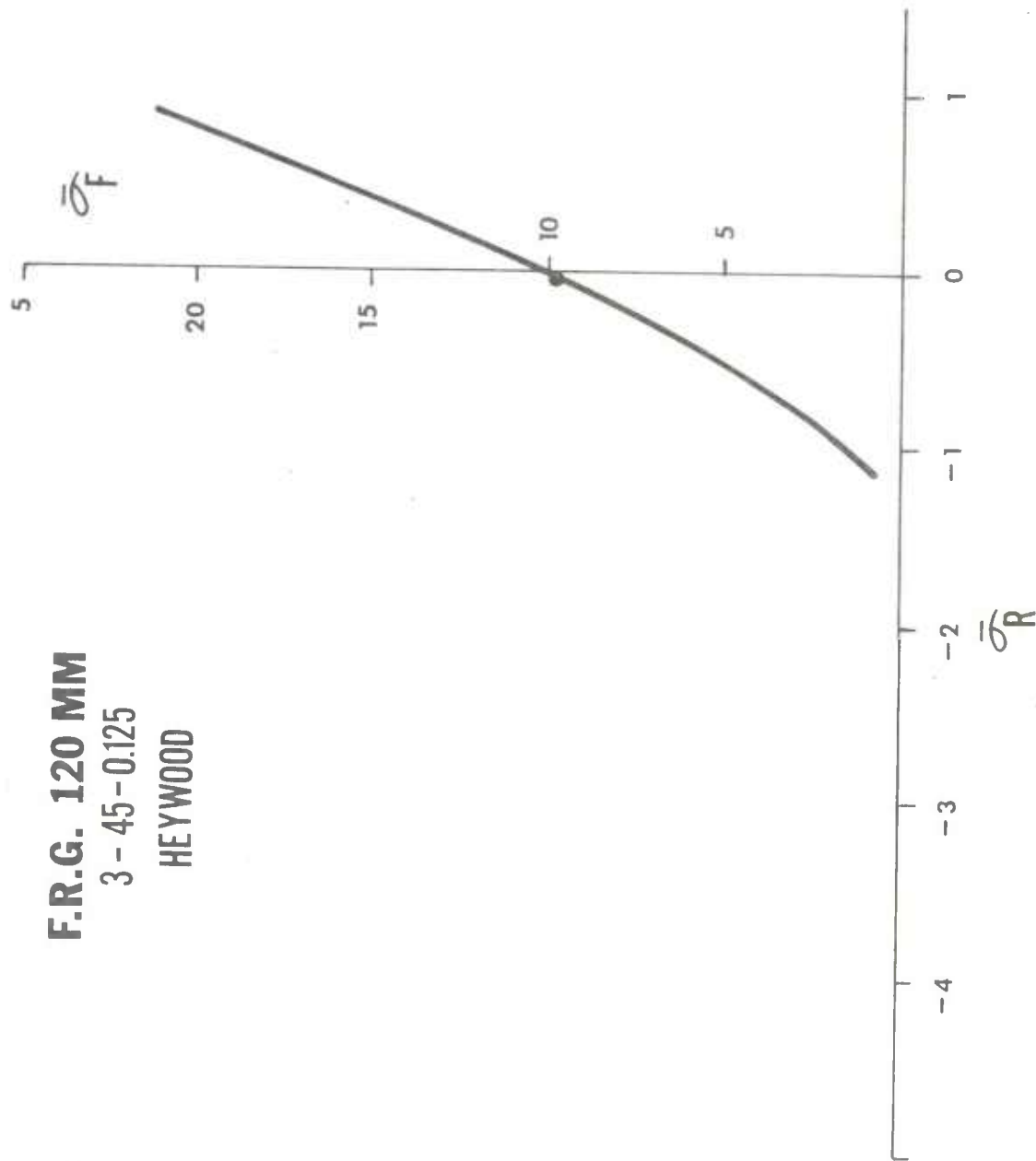


Figure A11. FRG 120 mm from Heywood.

WHITWORTH
 $27.5 - 27.5 - 0.137$
HEYWOOD

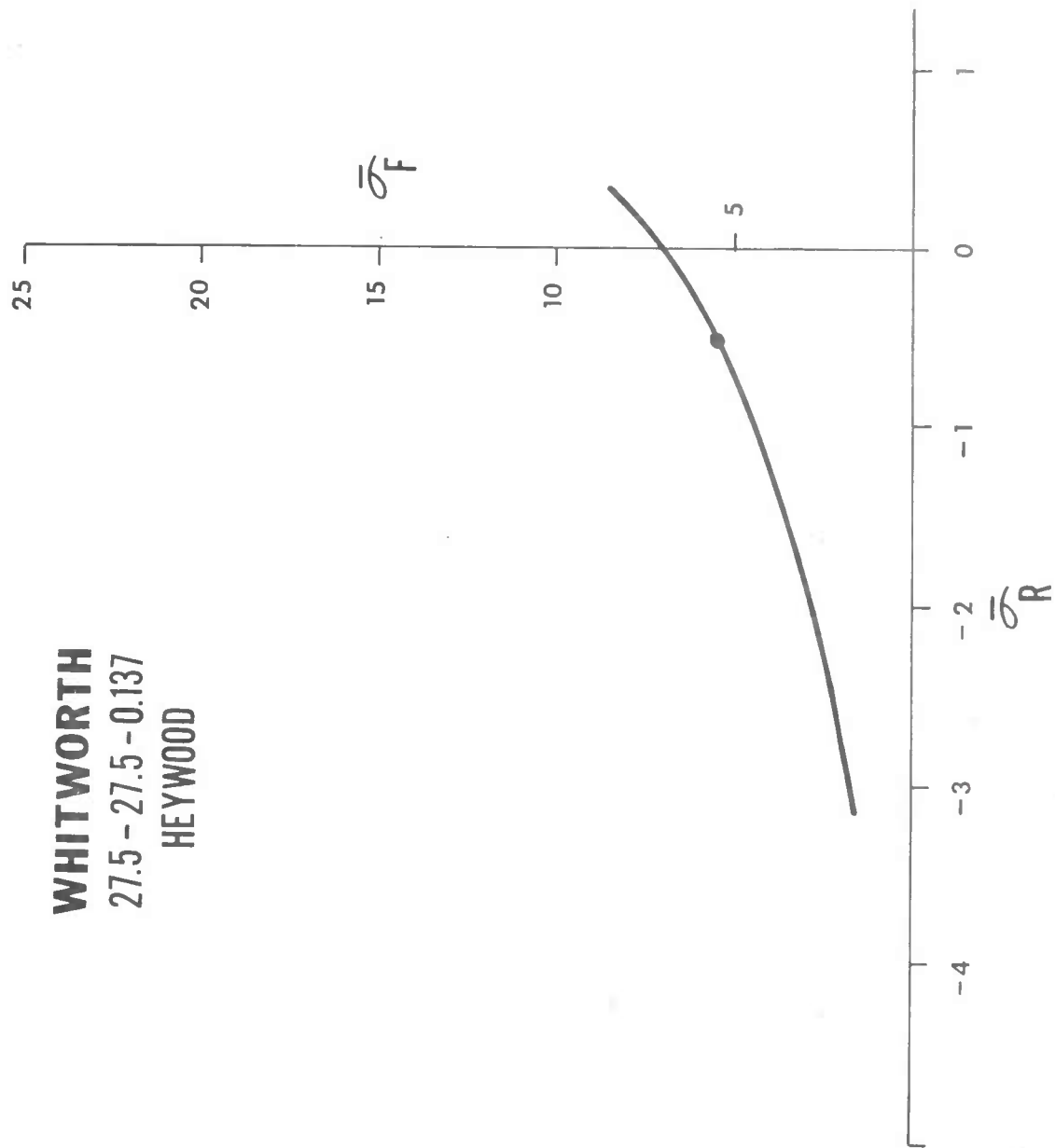


Figure A12. Whitworth from Heywood.

ISO STANDARD 'V'
30 - 30 - 0.144
HEYWOOD

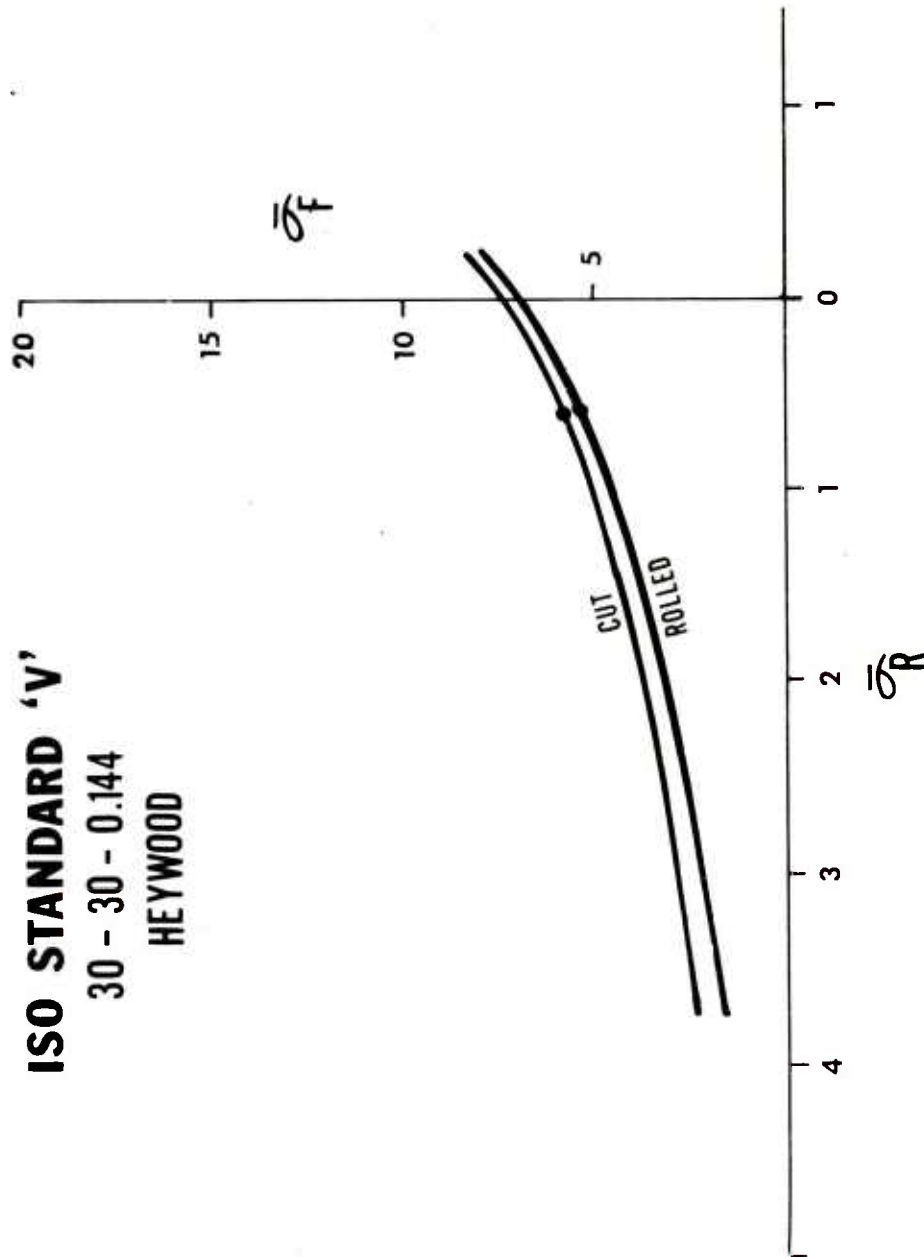


Figure A13. ISO Standard "V" cut and rolled from Heywood.

THREAD CHARACTERISTIC CURVE

CONTROLLED ROOT 'V' (UNJ)

FINATE ELEMENT ANALYSIS —

HEYWOOD'S EQUATION ---

$$\bar{\sigma}_a = 0.0$$

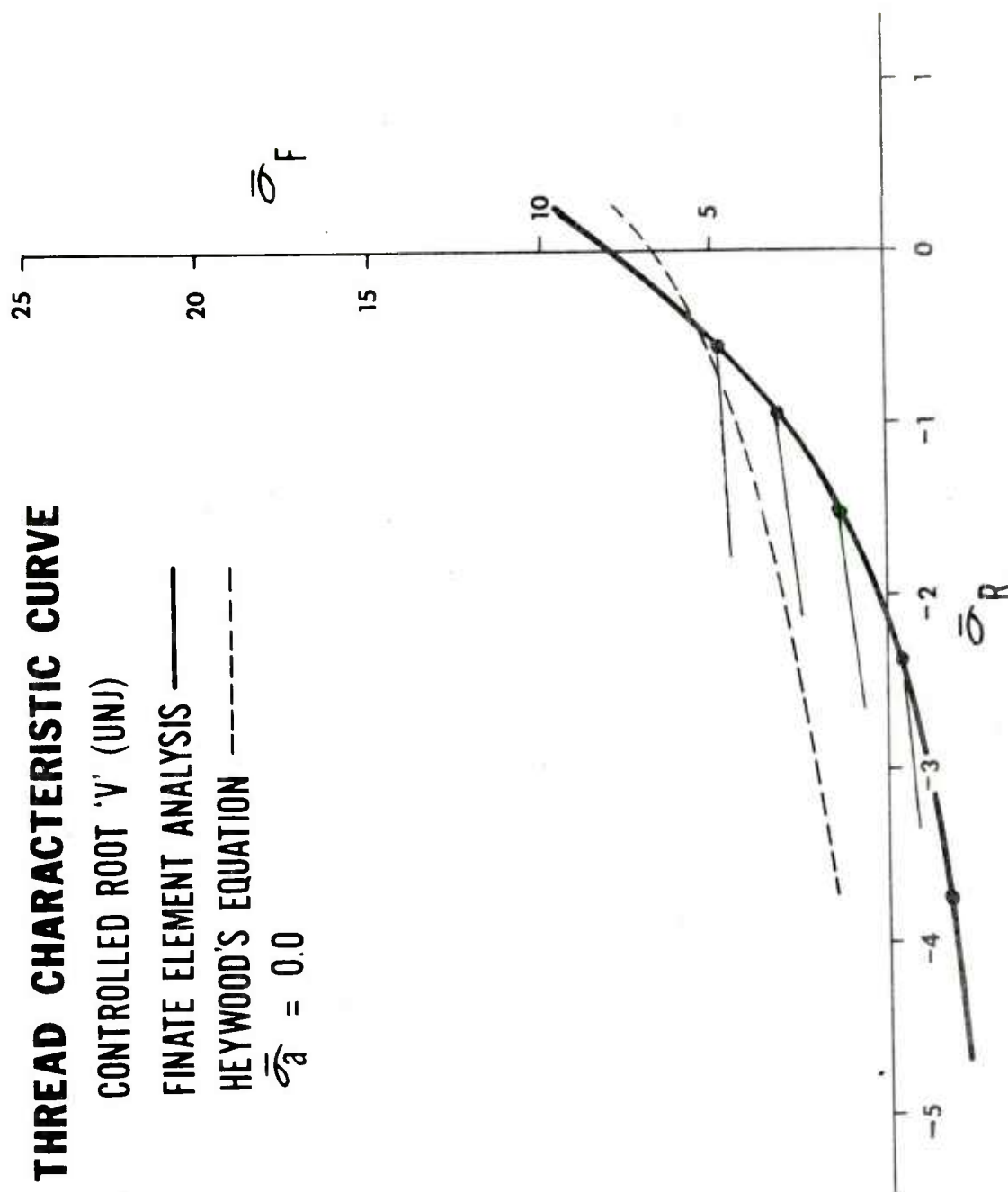


Figure A14. Controlled root "V" for axial stress of 0.0.

THREAD CHARACTERISTIC CURVE

CONTROLLED ROOT 'V' (UNJ)

FINITE ELEMENT ANALYSIS

$$\bar{\sigma}_a = 2.0$$

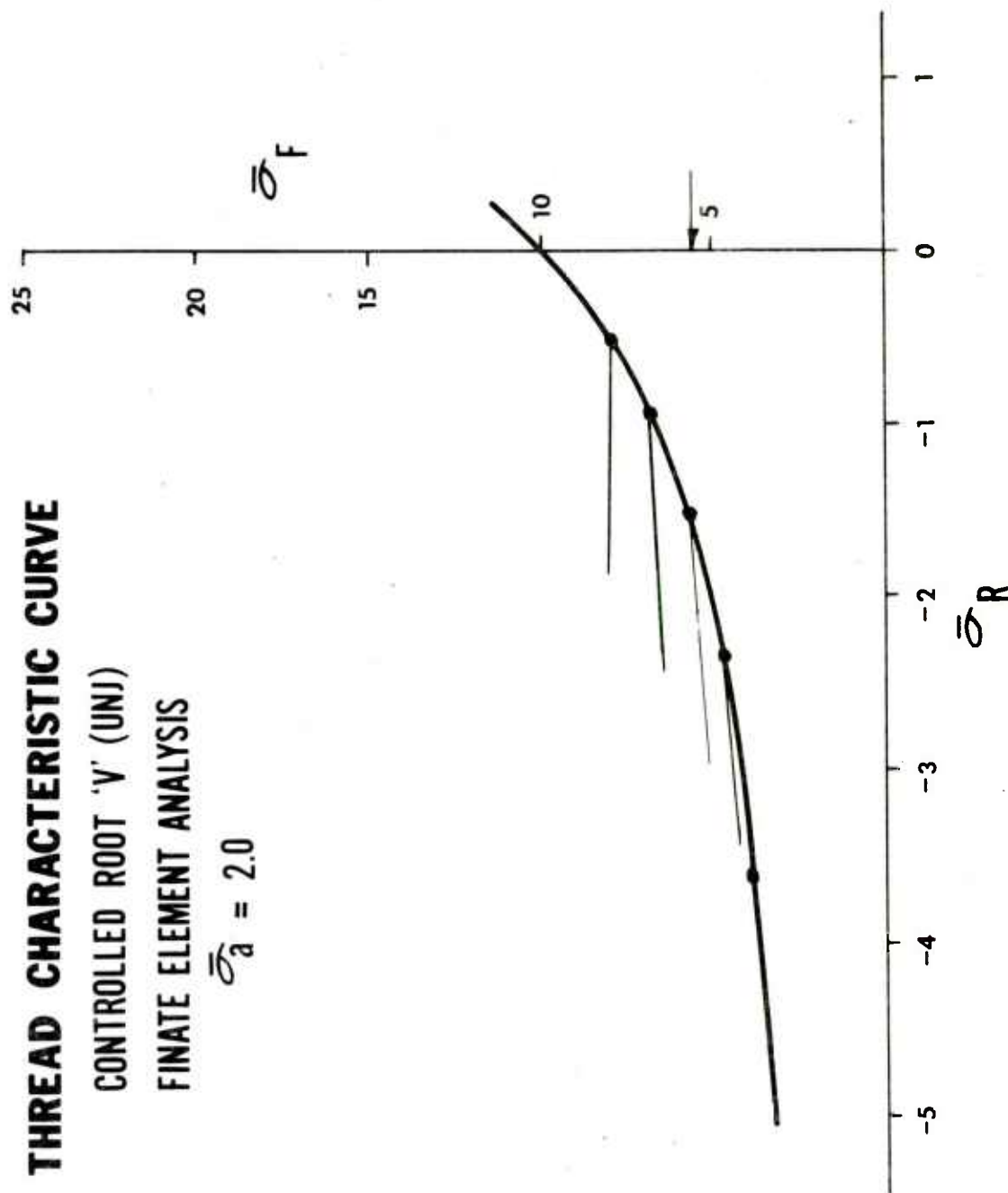


Figure A15. Controlled root "V" for axial stress of 2.0.

THREAD CHARACTERISTIC CURVE

CONTROLLED ROOT 'V' (UNJ)

FINITE ELEMENT ANALYSIS

$$\bar{\sigma}_a = 5.0$$

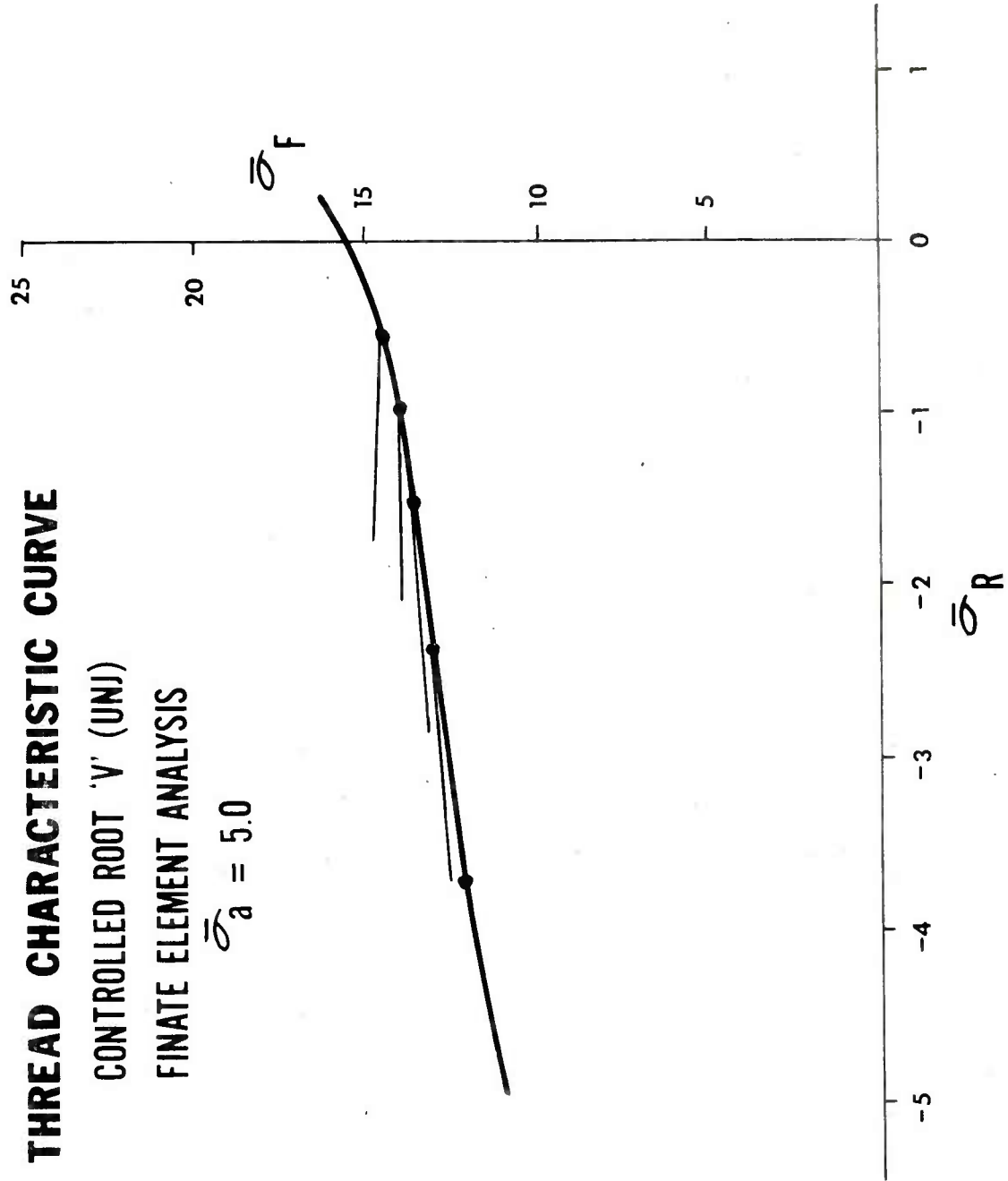


Figure A16. Controlled root "V" for axial stress of 5.0.

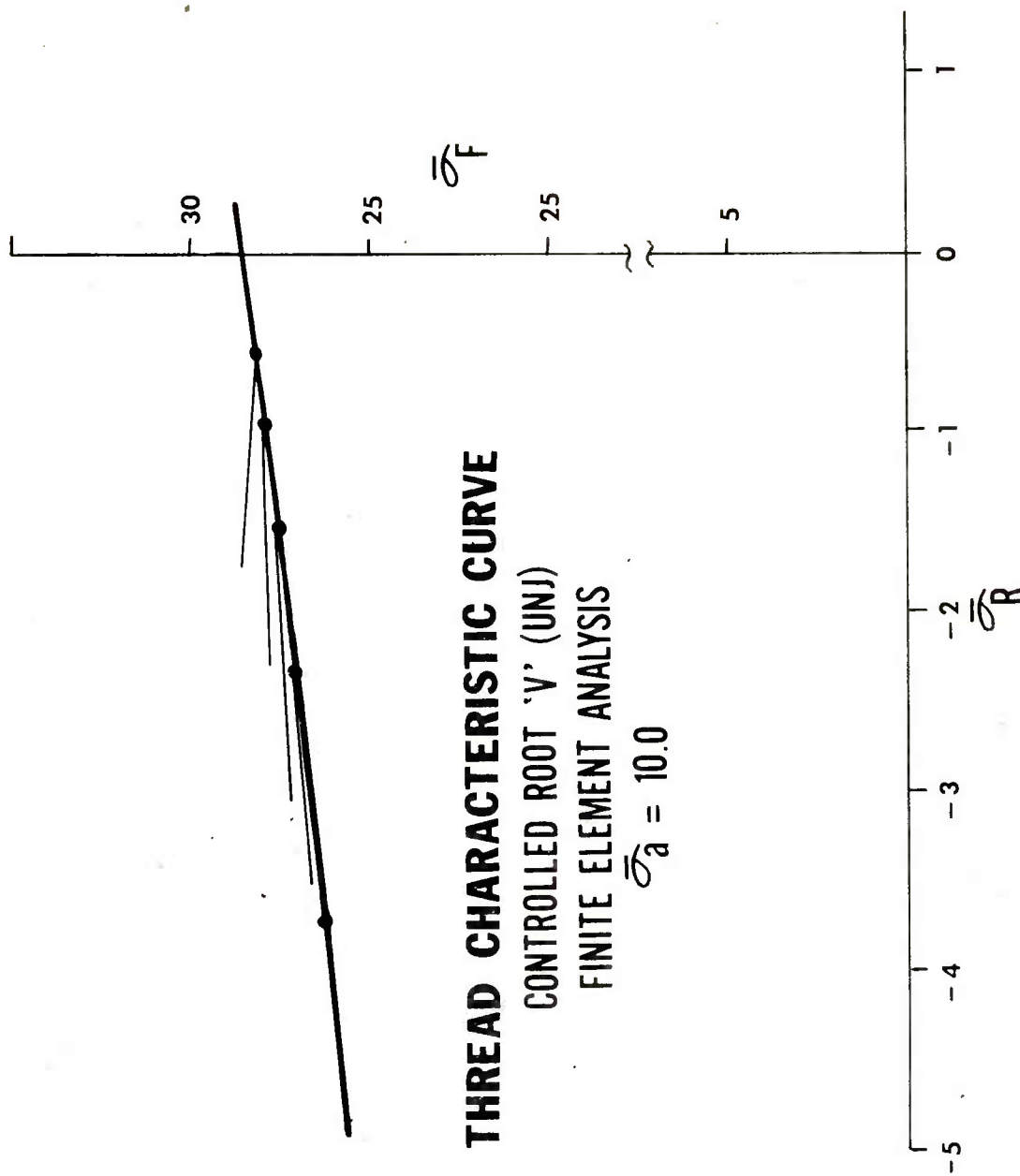


Figure A17. Controlled root "V" for axial stress of 10.0.

175 MM - 8 INCH BLOCK

35 - 35 - 0.120

HEYWOOD

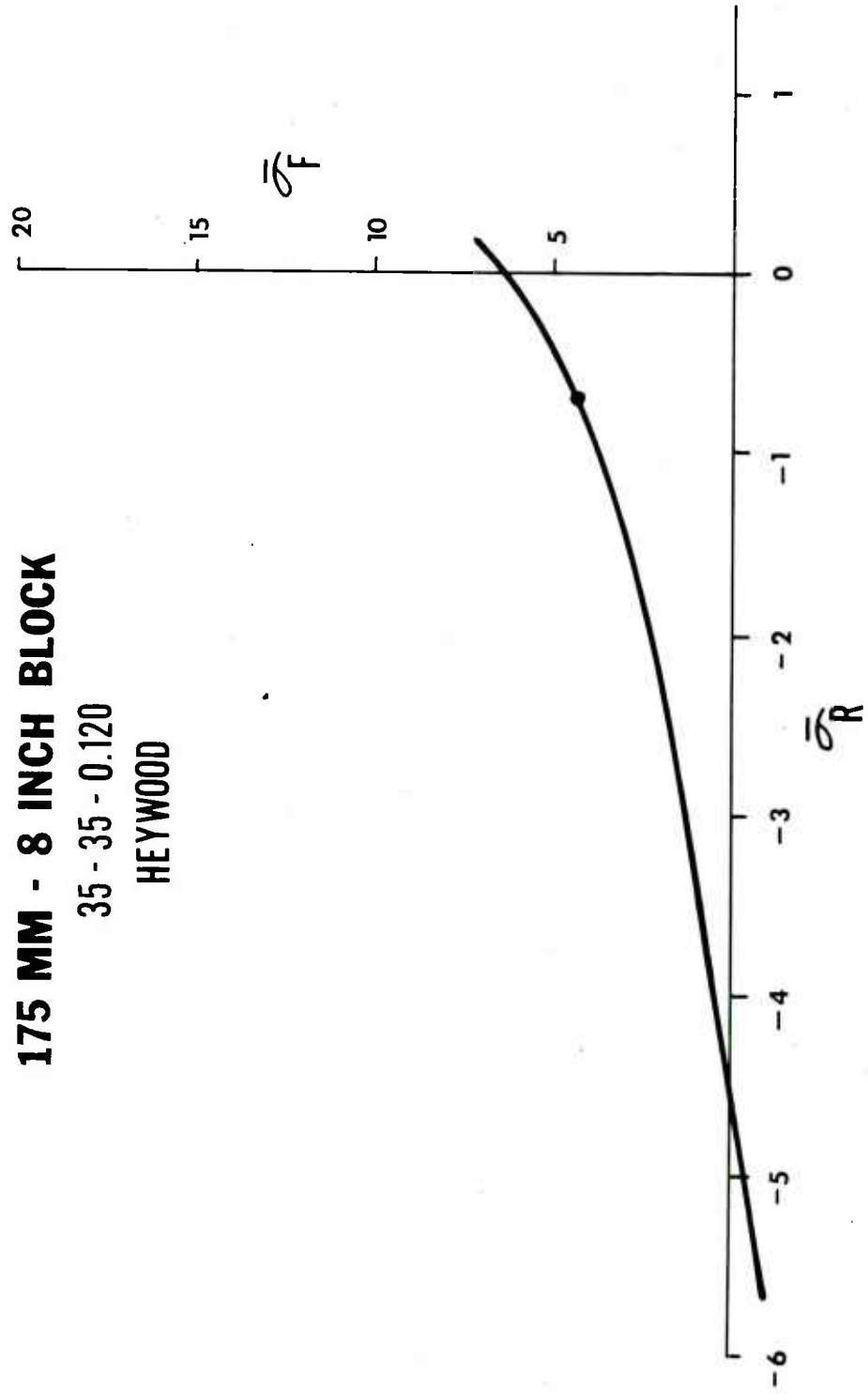


Figure A18. 175 mm - 8 Inch block from Heywood.

175 MM - 8 INCH BUSHING

15 - 37.15 - 0.136

HEYWOOD

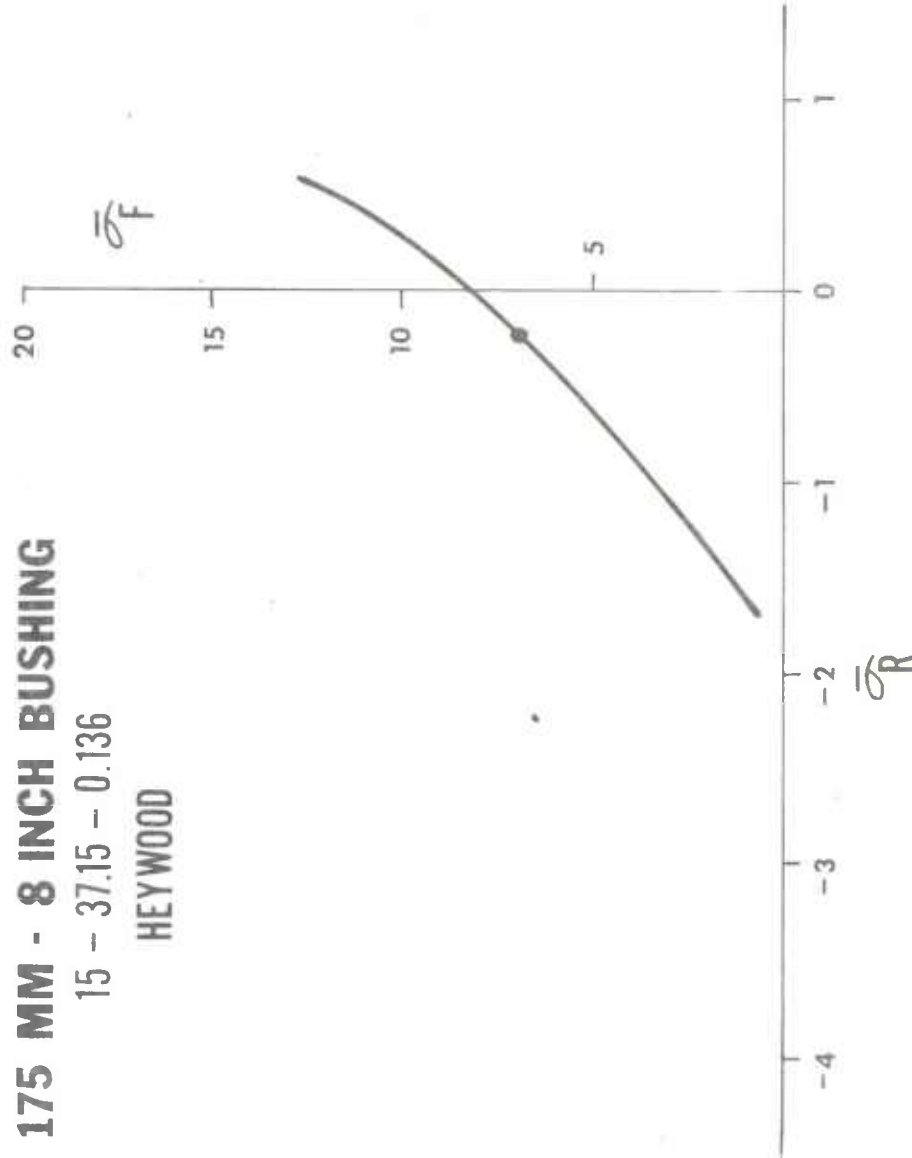


Figure A19. 175 mm - 8 Inch bushing from Heywood.

175 MM - 8 INCH TUBE

0.013
14.5 - 14.5 - 0.026

HEYWOOD

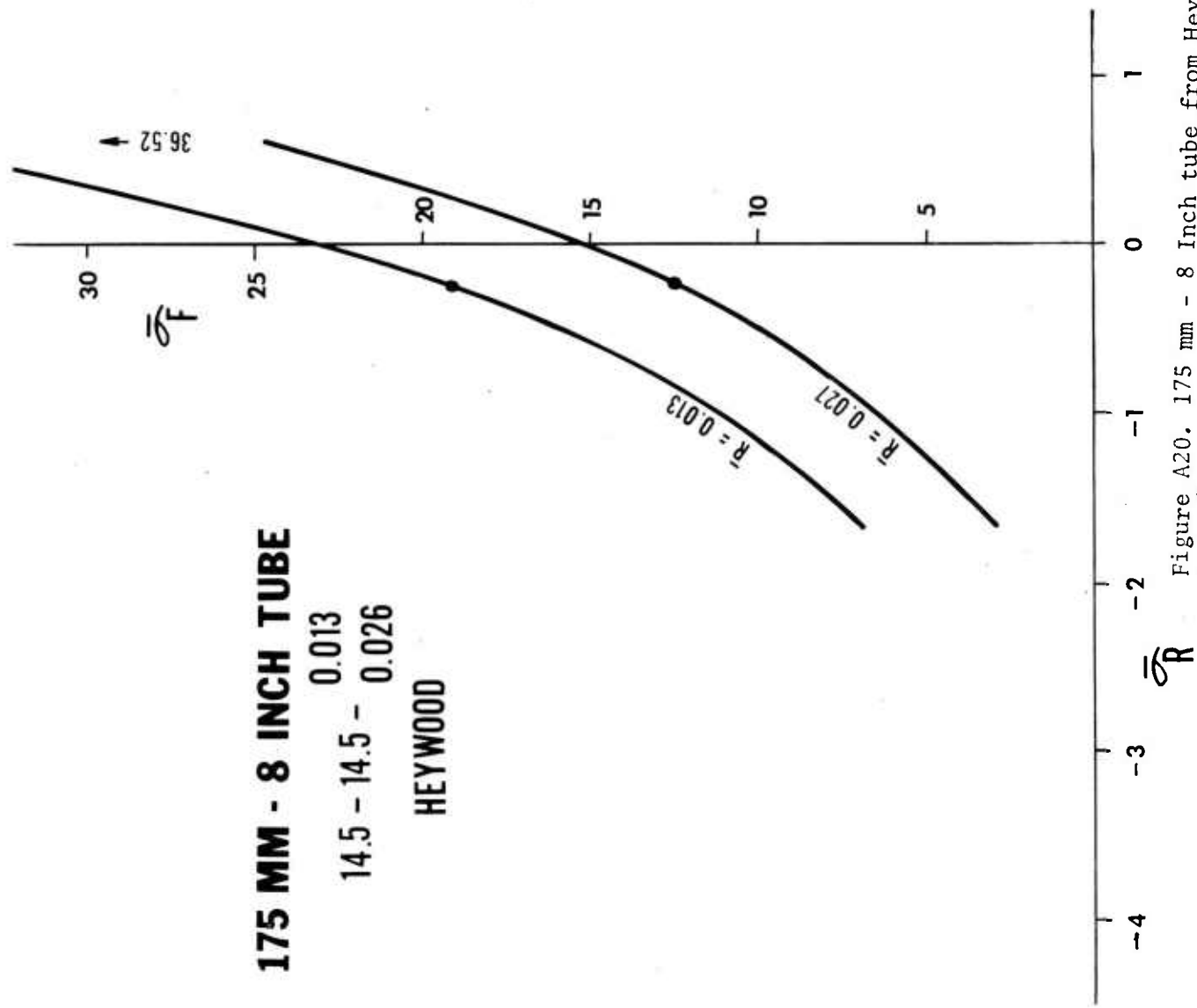


Figure A20. 175 mm - 8 Inch tube from Heywood.

TECHNICAL REPORT INTERNAL DISTRIBUTION LIST

	<u>NO. OF COPIES</u>
COMMANDER	1
CHIEF, DEVELOPMENT ENGINEERING BRANCH	1
ATTN: DRDAR-LCB-DA	1
-DM	1
-DP	1
-DR	1
-DS	1
-DC	1
CHIEF, ENGINEERING SUPPORT BRANCH	1
ATTN: DRDAR-LCB-SE	1
-SA	1
CHIEF, RESEARCH BRANCH	2
ATTN: DRDAR-LCB-RA	1
-RC	1
-RM	1
-RP	1
CHIEF, LWC MORTAR SYS. OFC.	1
ATTN: DRDAR-LCB-M	1
CHIEF, IMP. 81MM MORTAR OFC.	1
ATTN: DRDAR-LCB-I	1
TECHNICAL LIBRARY	5
ATTN: DRDAR-LCB-TL	
TECHNICAL PUBLICATIONS & EDITING UNIT	2
ATTN: DRDAR-LCB-TL	
DIRECTOR, OPERATIONS DIRECTORATE	1
DIRECTOR, PROCUREMENT DIRECTORATE	1
DIRECTOR, PRODUCE ASSURANCE DIRECTORATE	1

NOTE: PLEASE NOTIFY ASSOC. DIRECTOR, BENET WEAPONS LABORATORY, ATTN:
DRDAR-LCB-TL, OF ANY REQUIRED CHANGES.

TECHNICAL REPORT EXTERNAL DISTRIBUTION LIST

	<u>NO. OF COPIES</u>		<u>NO. OF COPIES</u>
ASST SEC OF THE ARMY RESEARCH & DEVELOPMENT ATTN: DEP FOR SCI & TECH THE PENTAGON WASHINGTON, D.C. 20315	1	COMMANDER US ARMY TANK-AUTMV R&D CMD ATTN: TECH LIB - DRDTA-UL MAT LAB - DRDTA-RK WARREN MICHIGAN 48090	1 1
COMMANDER US ARMY MAT DEV & READ. CMD ATTN: DRUDE 5001 EISENHOWER AVE ALEXANDRIA, VA 22333	1	COMMANDER US MILITARY ACADEMY ATTN: CHMN, MECH ENGR DEPT WEST POINT, NY 10996	1
COMMANDER US ARMY ARRADCOM ATTN: DRDAR-IC	1	COMMANDER REDSTONE ARSENAL ATTN: DRSMI-RB	2
-ICA (PLASTICS TECH EVAL CEN)	1	-RRS	1
-ICE	1	-RSM	1
-ICM	1	ALABAMA 35809	
-ICS	1	COMMANDER ROCK ISLAND ARSENAL	
-ICW	1	ATTN: SARRI-ENM (MAT SCI DIV)	1
-TSS(STINFO)	2	ROCK ISLAND, IL 61202	
DOVER, NJ 07801			
COMMANDER US ARMY ARRCOM ATTN: DRSAR-LEP-L	1	COMMANDER HQ, US ARMY AVN SCH ATTN: OFC OF THE LIBRARIAN FT RUCKER, ALABAMA 36362	1
ROCK ISLAND ARSENAL ROCK ISLAND, IL 61299			
DIRECTOR US Army Ballistic Research Laboratory ATTN: DRDAR-TSB-S (STINFO)	1	COMMANDER US ARMY FGN SCIENCE & TECH CEN ATTN: DRXST-SD	1
ABERDEEN PROVING GROUND, MD 21005		220 7TH STREET, N.E. CHARLOTTESVILLE, VA 22901	
COMMANDER US ARMY ELECTRONICS CMD ATTN: TECH LIB	1	COMMANDER US ARMY MATERIALS & MECHANICS RESEARCH CENTER ATTN: TECH LIB - DRXMR-PL	2
FT MONMOUTH, NJ 07703		WATERTOWN, MASS 02172	
COMMANDER US ARMY MOBILITY EQUIP R&D CMD ATTN: TECH LIB	1		
FT BELVOIR, VA 22060			

NOTE: PLEASE NOTIFY COMMANDER, ARRADCOM, ATTN: BENET WEAPONS LABORATORY, DRDAR-ICB-TL, WATERVLIET ARSENAL, WATERVLIET, N.Y. 12189, OF ANY REQUIRED CHANGES.

TECHNICAL REPORT EXTERNAL DISTRIBUTION LIST (CONT)

	NO. OF COPIES		NO. OF COPIES
COMMANDER US ARMY RESEARCH OFFICE P.O. BOX 12211 RESEARCH TRIANGLE PARK, NC 27709	1	COMMANDER DEFENSE TECHNICAL INFO CENTER ATTN: DTIA-TCA CAMERON STATION ALEXANDRIA, VA 22314	12
COMMANDER US ARMY HARRY DIAMOND LAB ATTN: TECH LIB 2800 POWDER MILL ROAD ADELPHIA, MD 20783	1	METALS & CERAMICS INFO CEN BATTELLE COLUMBUS LAB 505 KING AVE COLUMBUS, OHIO 43201	1
DIRECTOR US ARMY INDUSTRIAL BASE ENG ACT ATTN: DRXPE-MT ROCK ISLAND, IL 61201	1	MECHANICAL PROPERTIES DATA CTR BATTELLE COLUMBUS LAB 505 KING AVE COLUMBUS, OHIO 43201	1
CHIEF, MATERIALS BRANCH US ARMY R&S GROUP, EUR BOX 65, FPO N.Y. 09510	1	MATERIEL SYSTEMS ANALYSIS ACTV ATTN: DRXSY-MP ABERDEEN PROVING GROUND MARYLAND 21005	1
COMMANDER NAVAL SURFACE WEAPONS CEN ATTN: CHIEF, MAT SCIENCE DIV DAHLGREN, VA 22448	1		
DIRECTOR US NAVAL RESEARCH LAB ATTN: DIR, MECH DIV CODE 26-27 (DOC LIB) WASHINGTON, D. C. 20375	1 1		
NASA SCIENTIFIC & TECH INFO FAC P. O. BOX 8757, ATTN: ACQ BR BALTIMORE/WASHINGTON INTL AIRPORT MARYLAND 21240	1		

NOTE: PLEASE NOTIFY COMMANDER, ARRADCOM, ATTN: BENET WEAPONS LABORATORY,
DRDAR-LCB-TL, WATERVLIET ARSENAL, WATERVLIET, N.Y. 12189, OF ANY
REQUIRED CHANGES.